Phosphatidylcholine is organized in long-lived plasmalemmal platforms

Dissertation

zur

Erlangung des Doktorgrades (Dr. rer. nat.)

der

Mathematisch-Naturwissenschaftlichen Fakultät

der

Rheinischen Friedrich-Wilhelms-Universität Bonn

vorgelegt von

Luis Fernando Spitta

aus

La Ceiba, Honduras

Bonn 2012

Angefertigt mit der Genehmigung der Mathematisch-
Naturwissenschaftlichen Fakultät der Rheinischen Friedrich-Wilhelms-
Universität Bonn

1. Gutachter

Herr Prof. Dr. Thorsten Lang

2. Gutachter

Herr Prof. Dr. Christoph Thiele

Tag der Promotion: 16.01.2013

Erscheinungsjahr: 2013

Eidesstattliche Erklärung

Ich versichere, dass ich die vorgelegte Dissertation selbstständig und ohne unerlaubte Hilfe angefertigt habe. Diese Arbeit hat in gleicher oder ähnlicher Form noch keiner Prüfungsbehörde vorgelegen.

Bonn, den

Nachname: **Spitta** Vorname: **Luis Fernando**

Unterschrift:

Erklärung

Teile dieser Arbeit befinden sich im Prozess der Veröffentlichung:

Spitta, L.; Merklinger, E.; Saka-Kirli, S.; Schloetel, J.G.; Lauria, I.; Schmidt, T.H.; Kandt, C.; Rizzoli, S.O.; Thiele, C.; Lang, T. (2012): Long-lived supramolecular phosphatidyl-choline platforms in native membranes (submitted to Cell 09/2012).

Weitere erhobene Daten, die nicht im Rahmen des Themas der hier vorliegenden Dissertation diskutiert wurden, sind:

Zilly, F. E.; Halemani, N. D.; Walrafen, D.; **Spitta, L.**; Schreiber, A.; Jahn, R.; Lang, T. (2011): Ca^{2+} induces clustering of membrane proteins in the plasma membrane via electrostatic interactions. EMBO J 30 (7), S. 1209–1220.

Lauria, I.; van Üüm, J.; Mjumjunov, E.; Walrafen, D.; **Spitta, L.**; Thiele, C.; Lang, T. (2012): GLTP mediated non-vesicularGM1 transport between native membranes (accepted manuscript,Plos One 02/2013, manuscript no.: PONE-D-12-37467R1).

Lechner H.; Krsmanovic T.;**Spitta L.**; Lang T.; Hoch M.; Bauer R. (2012): Innexin oligomerization and trafficking to the plasma membrane (submitted to FEBS Letters 02/2013).

Table of contents

I. List of figures

II. List of Tables

III. List of abbreviations

Ab	antibody
Ac	acetate
AHT	anhydrotetracycline
a.u.	arbitrary units
BP	bandpass
BSA	bovine serum albumin
CCD	charged coupled device
CLSM	confocal laser scanning microscopy
DAPI	4',6-diamidino-2-phenylindol
ddH$_2$O	double distilled water
DMEM	Dulbecco's modified eagle medium
DMSO	dimethylsulfoxide
DNA	deoxyribonucleic acid
DRM	detergent resistant membrane
DTT	dithiothreitol
E.coli	*Escherichia coli*
EGTA	ethyleneglycol-bis-(2-aminoethylether)-N,N,N',N'-tetraacetic acid
EMEM	Eagle's minimal essential medium
EtOH	ethanol absolute
EGFP	enhanced green fluorescent protein
FBS	fetal bovine serum
FCS	fluorescence correlation spectroscopy
FRAP	fluorescence recovery after photobleaching
FRET	Förster resonance energy transfer
FWHM	full width at half maximum

g	gramm
Glc	glucose
Gln	glutamine
Glu	glutamate
GP	glycerophospholipids
h	hour
Hz	Hertz
kDa	kilo Dalton
L	liter
MeOH	methanol
MβCD	methyl-β-cyclodextrin
min	minute
ms	millisecond
NA	numerical aperture
ON	over night
PBS	phosphate buffered saline
PC12	Pheochromocytoma cells
PCR	polymerase chain reaction
PFA	paraformaldehyde
pH	negative logarithm of H^+ concentration
PLL	poly-L-lysine
PM	plasma membrane
PC	phosphatidylcholine
pPC	propargyl-phosphatidylcholine
PSF	point spread function
ROI	region of interest
rpm	rounds per minute

RT	room temperature
s	second
SD	standard deviation
SDS	sodium dodecyl sulfate
SEM	standard error of the mean
SM	sphingomyelin
SNARE	*soluble N-ethylmaleimide-sensitive-Factor attachement receptor*
SNAP23	*synaptosomal-associated protein* of 23kDa
SNAP25	*synaptosomal-associated protein* of 25kDa
SP	sphingophospholipids
Syx	s*yntaxin*
STD	standard deviation
STED	stimulated emission depletion
TLC	thin layer chromatography
TIRF	total internal reflection fluorescence
TMA-DPH	1-(4-Trimethyl-ammoniumphenyl)-6-Phenyl-1,3,5-Hexatriene-p-toluolsulfonate
TMR (TMD)	transmembrane region (domain)
vs.	versus
v/v	volume / volume
w/v	weight / volume
xg	relative centrifugal force

IV. Zusammenfassung

Lebende Zellen sind umhüllt von einer Zellmembran, welche aus Proteinen und Lipiden besteht. Die laterale Organisation dieser Bausteine innerhalb der Zellmembran ist Gegenstand aktueller Forschung. So wird z.B. seit zwei Dekaden diskutiert ob Lipide stabile Assemblate, Domänen oder Plattformen in der Zellmembran bilden können.

Ein grundsätzliches Problem bei der Aufklärung dieser Fragen besteht in der Visualisierung von Lipidstrukturen. Das Lipid Phosphatidylcholin (PC) gehört zu den verbreitesten Lipiden in Zellmembranen. Seit kurzem besteht die Möglichkeit, PC nach nicht-invasiver metabolischer Markierung gefolgt von Fluoreszenzmarkierung in Membranen sichtbar zu machen.

In der vorliegendenArbeitwurde eine Kombination dieser eleganten, nicht invasiven Markierung und verschiedene moderne Methoden aus der Mikroskopie angewendet, um die Verteilung des Lipides innerhalb der Plasmamembran zu untersuchen. Für die Analysen wurden sowohl ganze Zellen als auch zellkörperfreie Plasmamembranpräparationen, sogenannte „Membrane Sheets" untersucht. Es konnte nicht nur wie erwartet eine homogene Verteilung von PC innerhalb der Plasmamembran beobachtet werden, sondern es wurden auch lokal begrenzte PC-Plattformen entdeckt. Die PC-Domänen wurden charakterisiert durch Vermessung ihrer Größe und der Berechnung des Anreicherungsfaktors vom Lipid gegenüber der homogenen Membranumgebung. Ferner konnte auch gezeigt werden, dass obwohl diese PC-Domänen im Mittel nicht in der Molekülanzahl fluktuieren dennoch Lipide mit ihrer Umgebung austauschen.

Anhand von den erhobenen Ergebnissen und den erarbeiteten Resultaten aus Kollaborationen wurde ein Modell entwickelt, welches einen konzeptionellen Rahmen für die Organisation von PC innerhalb der Plasmamembran liefert. Das Modell suggeriert, dass PC

Lipidplattfomen einen Durchmesser von 120 nm besitzen und aus rund 20000 PC-Molekülenbestehen,wobei PC 50 % der Plattformoberfläche bedeckt. Die Ergebnisse dieser Arbeit sind aus zellbiologischem Standpunkt weitreichend bedeutend, da bis jetzt keine Lipidplattformen innerhalb von Zellmembranen auf diesem Niveau charakterisiert werden konnten. Somit kann zu der oben genannten Diskussion ein essentieller Beitrag geliefert werden, indem bestätigt wird, dass Lipidplattformen existieren.

V. Summary

All living cells are enclosed by a membrane that is mainly made up of proteins and lipids. The lateral organization of these constituents is a subject in current research. Ithas beendiscussed since two decades whether lipids are able to form stable assemblies, domains or platforms in the plasma membrane.

A major issuein this fieldis the visualization of lipid structures. The lipid phosphatidylcholine (PC) is one of the most common lipids in the plasma membrane. Recently, PC was visualized in membranes via a non-invasive metabolic labeling followed by fluorescent labeling.

In the present work, the arrangement of this lipid within the plasma membrane was studied using a combination of this elegant, non-invasive labeling and a variety of modern fluorescent microscopy techniques. Both whole cells as well as cell body free plasma membrane preparations, so-called "membrane sheets", were used for the analyses. It was demonstrated that PC is not only homogenouslyfound within the plasma membrane, but also organized into locally restricted lipid platforms. The PC domains were characterized by determining their size and calculating the enrichment factor of the lipid in these spots in comparison to their homogenous surrounding. Furthermore, it could be demonstrated that although these PC-enriched structures were not fluctuating in their number of molecules, they exchanged lipids with their surroundings.

Based on thisstudy and together with acquired results from collaborators, a model was developed that broadens the current view of the organization of PC within the plasma membrane. PC platforms have been calculated to have a diameter of 120 nm, consist of about 20,000 lipids and PC comprises 50 % of the platform. So far, lipid platforms on the plasma membrane could not be visualized and characterized. Hence, this work is of essential importance for the cell biological field validating the existence of lipid platforms.

1.   Introduction

1.1   The theory of the cell

The definition of the cell was established in 1664 when Robert Hooke first described what he saw in a cork sample with the help of a very rudimentary and simple microscopy setup. He could observe "little chambers", as he called them, and therefore he used the Latin name *cellula* (=cell)(Hooke, 1664). With the advancements ofoptics in the microscope setups in those early years, it was then in 1838 when Matthias Schleiden and Theodor Schwann after studying samples from plants and animals both first established the differences and proposed a general cell theory: "All living things are composed of cells that have analogue structures and cells are the basic unit of life" (Schleiden, 1838;Schwann et al., 1847).
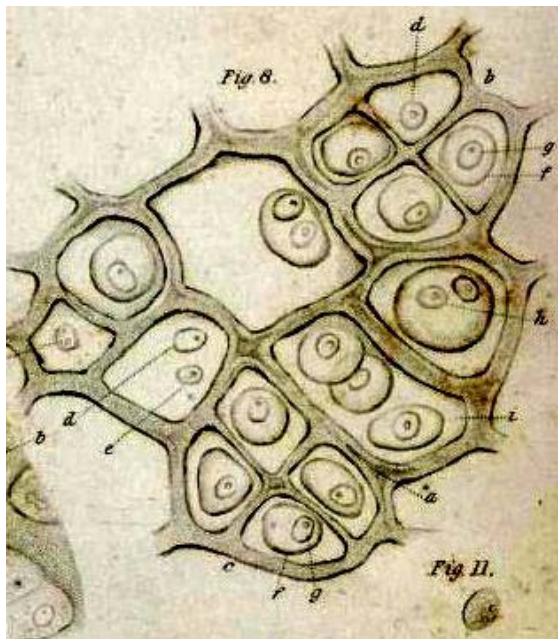
Figure1: Cells recognized by Theodor Schwann.
Branchial cartilage from the larva of Rana esculenta (modified fromSchwann et al., 1847)
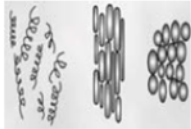
Rudolf Virchow described a few years later that cells divide and that every single cell is derived from a pre-existing cell (Virchow, 1871). The aspects postulated by the three lastly named scientists accredited them with the cell theory, since their announcements for our comprehension of a cell are valid until today.

1.2 Biological membranes

Biological membranes are fundamental to life because they enclose, separate and define cells and organisms (Table 1). Theyalso play an important role in defining membrane organelles within eukaryotic cells e.g. the endoplasmic reticulum (ER), the nuclear envelope or organelles like mitochondria and lysosomes. A consequence of compartmentalization are several functionsconferred to the membranes e.g. providing cells with energy derived from chemical and charge gradients (Batista et al., 2012) or mediating the transduction of information via receptors found on the plasma membrane(Akira and Takeda, 2004). Another important feature is the selective permeability of the plasma membrane of cells that allows movement of specific ions and organic molecules in and out of the cell e.g. uptake of nutrients is regulated and most harmful agents are excluded from entering the cell.

Table 1. Distinct biological membranes found in organisms.
Correlation between lipid compositional complexity and cellular architecture and function (Lipids: phosphatidylethanolamine (PE), phosphatidylglycerol (PG), sphingolipids (SP), glycerophospholipids (GP) (modified from Simons and Sampaio, 2011).

	Bacteria	Yeast	Higher Organisms
Lipid Composition	Mainly PE and PG	4 SPs, GPs and sterols	Gps, sterols and tissue specific SPs
Membrane Properties	Robust, different shapes	Robust, different shapes, complex organelle morphology	Robust, different shapes, complex organelle morphology, complex and specific cellular architecture
Functionalities	Membrane protein incorporation	Membrane protein incorporation, membrane budding, vesicular trafficking	Membrane protein incorporation, membrane budding, vesicular trafficking, specific functions depending on the cell type

Biological membranes are bilayers formed by lipids that embed proteins in a lipid matrix.

1.3 The plasma membrane of eukaryotic cells and its composition

The plasma membrane of eukaryotic cells separates the inside of a cell from its environment and is composed of more or less defined composition regarding lipids, proteins and carbohydrates (Phillips et al., 2009; Ohtsubo and Marth, 2006).

Lipids are amphipathic molecules thatvary in their chemical structure. A cell is capable of metabolizing more than 1000 distinct lipids (van Meer et al., 2008) being able to combine distinct head groups with acyl chains of different lengths. Lipids tend to self-associate in aqueous solution and arrange in the energetically most efficient orientation.
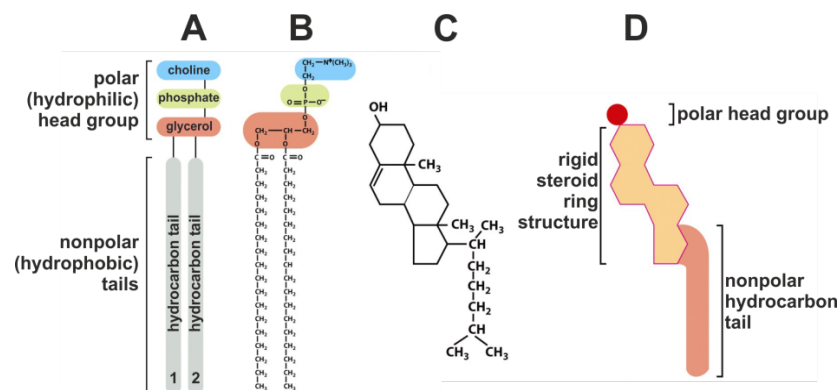
Figure 2. Two major lipids found in the PM of cells. Phosphatidylcholine (schematical (A) and chemical formula (B)), the most abundant phospholipid in cell membranes, and cholesterol (formula (C) and scheme (D)), another important component of the PM (modified from Alberts, 2008).

The polar headgroups of the lipids point towards the aqueous environment, while their acyl chains form a non-polar environment in between.Phospholipids are the largest group of related lipids within the plasma membrane, followed by sphingolipids and sterols (van Meer et al., 2008).

Proteins that are embedded within the lipid bilayer are called integral membrane proteins. They have one or several transmembrane domains

that serve as anchor to the membrane. The epitopes of most proteins can be found at the intracellular leafletwhile some are only exposed to the outer part of the membrane. But there are also periphericmembrane-associated proteins that bind to the plasma membrane (Figure 3).
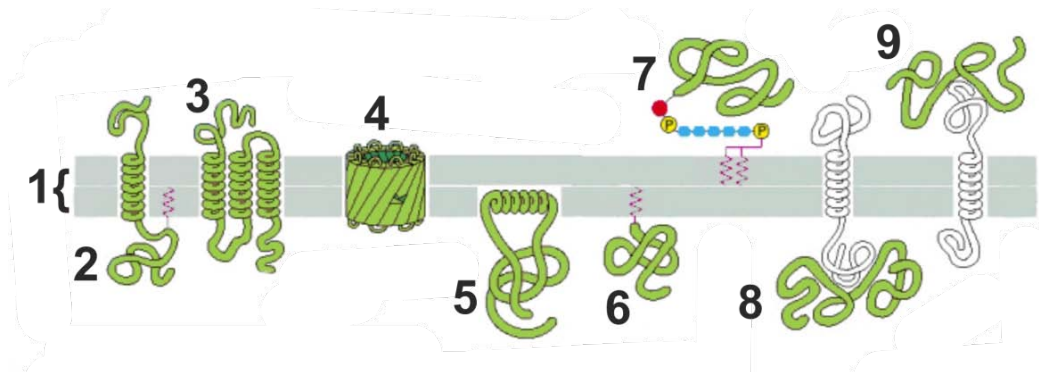
Figure 3.Association of proteins to the plasma membrane.
Proteins associate to the lipid bilayer (1) in different ways: transmembrane proteins with a single α-helix (2) or multiple α-helices (3) extend across the bilayer or as a rolled-up β-sheet as in the case of many channels (4). Other membrane proteins are present only on one side of the membrane and they are either bound by an amphipathic α-helix (5), by a covalently attached lipid chain (6) or even at the extracellular leaflet bound via an oligosaccharide linker (7). Proteins are also bound to other proteins by non-covalent interactions (8, 9)(modified from Alberts, 2008).

Both lipids and proteins can be modified during synthesis by attachment of carbohydrates. The glycosylated lipids or proteinsform another major constituent of the plasma membrane. They are exclusively found on the extracellular leaflet.

In summary, the three constituentsdictate the architecture of the plasma membrane(Figure 4) and its functional properties. Besides its role within the cell metabolism by maintaining charge and concentration gradients, a plasma membrane is also very active, flexible and self-healing. It is even maintained and repaired when needed during exo-/endocytotic processes (McNeil and Steinhardt, 2003). It is a dynamic structure with constant motion that houses different constituents that arrange and interact with each other. Within the last decades the interest for understanding the concept of this fundamental architecture for life has

increased. The research in this field developed different scientific paradigms that still bear many unknowns to science.
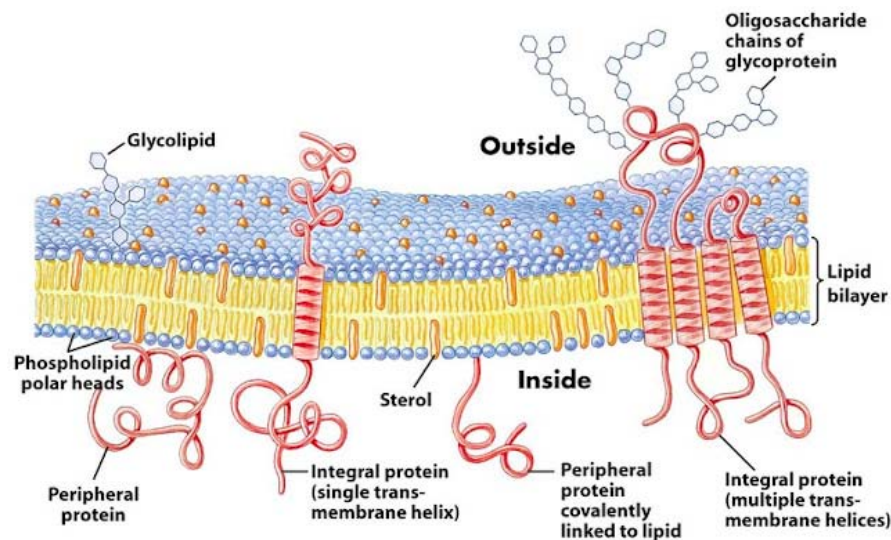
Figure 4.Membrane of cells. Simple scheme of the composition of the plasma membrane of eukaryotic cells (modified from Nelson et al., 2001).

1.4 Historical and current models of the plasma membrane

1.4.1 Historical models

The view of the plasma membrane of cells has been a very variable one. It has developed within the last century.The first researchers working on membranesstated that the PM must be a membrane composed of lipids and that lipids form a lipid bilayer (Overton, 1895;Gorter and Grendel, 1925). In their interpretations only little was mentioned about proteins in the lipid plasma membrane.

The first published model that was accepted dates to 1935 and was proposed by Danielliand Davson (Danielli and Davson, 1935). Their model of the membrane was based on thermodynamic argumentation and measurements of the surface tension ending up in a plasma membrane model in which proteins form globules on top and bottom of the lipid bilayer (Figure 5A). In 1959, Robertson used his observations established by thin section electron microscopy for arguing that the

proteins form a layer covering the lipid bilayer that looked like "a railroad track" (Figure 5B;Robertson, 1981). Another model proposed by Benson and Green (Figure 5C, Aloia, 1983) is the opposite of the models previously described showing a membrane in which proteins are solvated by lipids. This model never gained major acceptance.
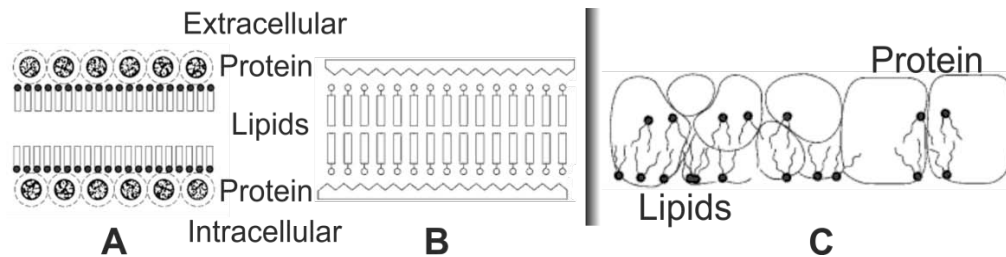
Figure 5. Historical models of membrane organization.
According to Danielli and Davson, the lipids are surrounded by proteins arranged as globular packages on top of the bilayer (A). Robertson's model basically modified the protein arrangement, by proposing that they are like a railroad track aligning the lipids (B). The opposite of the mentioned models was proposed by Benson and Green (C) showing protein particles that are solvated by lipids and readily fractionated into complexes (modified from 1935; Robertson, 1981;Aloia, 1983).

1.4.2 The fluid mosaic model

While in both (Danielli and Davson model and the Robertson model) the nature of the lipid bilayer was correctly described, their concept was still poor regarding the incorporation of proteins into the bilayer. In this respect,in 1972S.J. Singer and G. L. Nicolson revolutionizedthe previous conception with their fluid mosaic model (Figure 6). It summarizes the outcome of several experiments concerning the energetic behavior of proteins and lipids and their association to each otherwhen forming the plasma membrane of cells. Singer and Nicolson describe the PM as a fluid phospholipid matrix that contains a mosaic of proteins.The matrix allows a lateral diffusion, so dynamic plays an important role in distribution of the different constituents of the PM. The fluidic properties were shown in 1970 by fusing two mammalian cells (Frye and Edidin, 1970). The new postulated model could answer e.g. that some proteins are embedded within the PM and have

transmembrane domains that allow them to pass the membrane or the question about the thickness of the membrane. This model became the basis forthe scientific community that has been constantly modified andadapted according to recent findings concerning membrane organization.
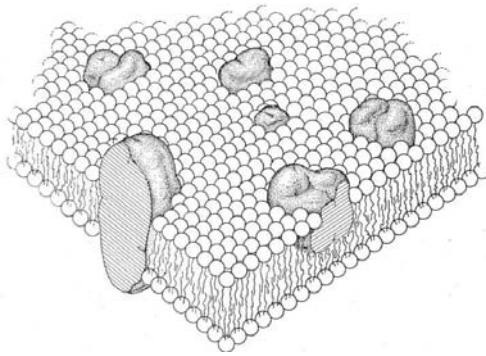
Figure 6.The fluid mosaic model.Model of the plasma membrane proposed by Singer and Nicolsonin 1972. Membrane proteins are embedded in the lipid bilayer. (modifiedfrom Singer and Nicolson, 1972)

1.4.3The anchored transmembrane protein picket fence model

In the fluid mosaic model, proteins diffuse freely along the PM. However, experimental data has shown that proteins are generally restricted in mobility. One possibility for obstructions is the cytoskeleton. Results obtained by experiments performed on diffusion of proteins on the membrane of erythrocytes showed that the cytoskeleton has an influence on lateral diffusion (Sheetz et al., 1980).The next generated model, the so called picket fence model, arose after clarifying that lateral movement of proteins seems to be affected by different factors. Sheetz continued to analyze the diffusion within the "compartments" as he called the regions enclosing proteins and lipidsandargued that the cytoskeleton might act as a fence preventing a free lateral movement of proteins on the PM. Later, it wasshown that a degradation of the cytoskeleton by treatment with e.g.trypsin or Latrunculin B led to facilitated diffusion of proteins on the PM (Tsuji and Ohnishi, 1986, Cha et al., 2004).The area for the diffusion of proteins was calculated, defining the compartments to a size of about 230 nm diameters (Fujiwara et al., 2002). The expanded picket fence model is known

today as the anchored transmembrane protein picket fence model(Kusumi et al., 2005).It took into account that lipids are also hindered in diffusion across the PM by proteins that cross the PM and therefore create a barrier not only for the proteins but also for the rapid lipids.Fujiwara proposed that lipids are even able to travel between the compartments by hopping from one field to another (Fujiwara et al., 2002). The size of the compartments described by Fujiwara were confirmed by Morone demonstrating by electron micrographs the dense cytoskeleton (Figure 7) that lines the inner face of the PM (Morone et al., 2006).
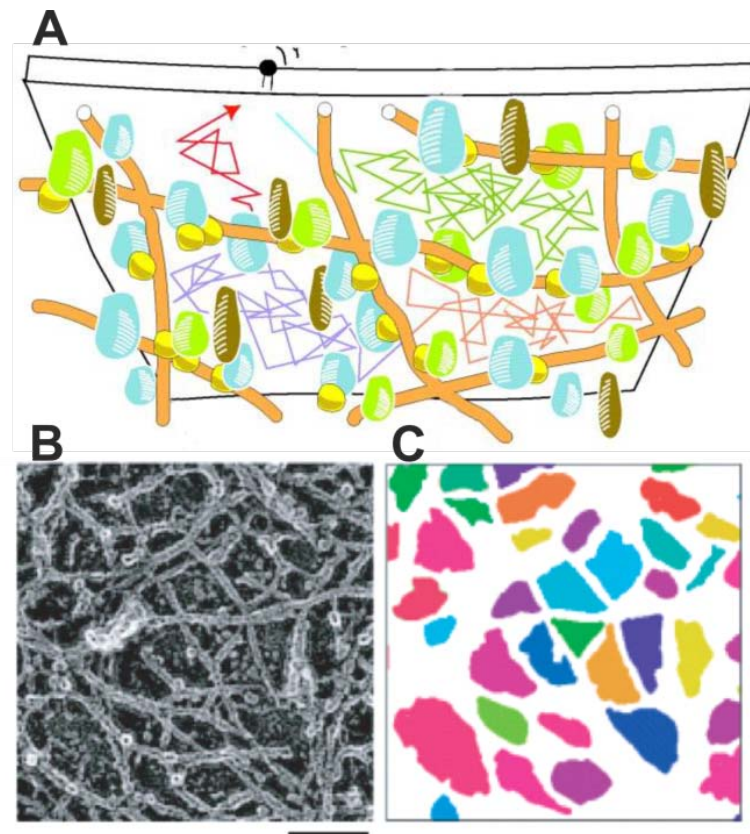
Figure 7.The anchored transmembrane protein picket fence model.
Model showing the diffusion tracks of a phospholipid within the fence created by the cytoskeleton (A) and anchored proteins. The original picket fence model was expanded after gaining experimental evidence that anchored proteins also act as barriers providing the pickets to the fence. The lower panel shows an electron micrograph of the dense cytoskeleton (B) and for better visualization by the eye, a coloration of the free space within the cytoskeleton (C). The scale bar in B represents 100 nm(Modified fromFujiwara et al., 2002;Morone et al., 2008).

1.4.4Membrane raft hypothesis

The picket fence model provides a reasonable explanation for observation of restricted diffusion within the PM.Alternatively the assembly of lipids within the plasma membrane into liquid ordered phases provided another concept for membrane compartmentalization. In the so-called*lipid raft* hypothesis (Simons and Ikonen, 1997), lipids interactand self-arrange intospecific microdomains resembling liquid-ordered phases known from model membranes.Simons and Ikonen postulated that the domains are created by clustering of sphingomyelin and cholesterol in the outer plasmalemmal leaflet to which specific raft proteins are recruited. These platforms enable functions like signaling, exo- and endocytosis (Rosa and Fratangeli, 2010; Gupta and DeFranco, 2007) or are even responsible for e.g. insulin resistance (Holzer et al., 2011). The existence of *lipid rafts* was first described upon the simple fact that cells lysed bythe detergent Triton-X100yieldeddetergent resistant membranes that could be isolated after density gradient centrifugation.This detergent resistant lipid rafts could be also found in specific model membranes with lipid concentrations and the concept of liquid ordered phases was established. Later,it was suggestedthat this liquid ordered phases were not only present in model membranes but also in native membranes.Within these phases, specific proteins were found and claimed to be specific markers for the lipid rafts (Foster et al., 2003). This argumentation for detection of rafts, became the major critical point because it was demonstrated by other experiments that treatment of the cells by detergent, generated such phases (Heerklotz, 2002;Shogomori and Brown, 2003;Zurzolo et al., 2003) and the rafts as they were first seen are only artifacts of this treatment. Until today, no evidence for liquid ordered phases has been observedin vivo (Mishra and Joshi, 2007; Hancock, 2006).Nevertheless, the concept was not withdrawn. In 2006, the Keystone Symposium defined new characteristics for the exact description of membrane rafts –as they were newly named (Pike, 2006).They were declared to be highly dynamic platforms of 10-200 nm in size, heterogeneous layers

made from sphingomyelin and sterols that are able to (de-)arrange quickly and serve as enriched platforms for lipid-lipid, lipid-protein or even protein-protein interactions (Simons and Gerl, 2010).
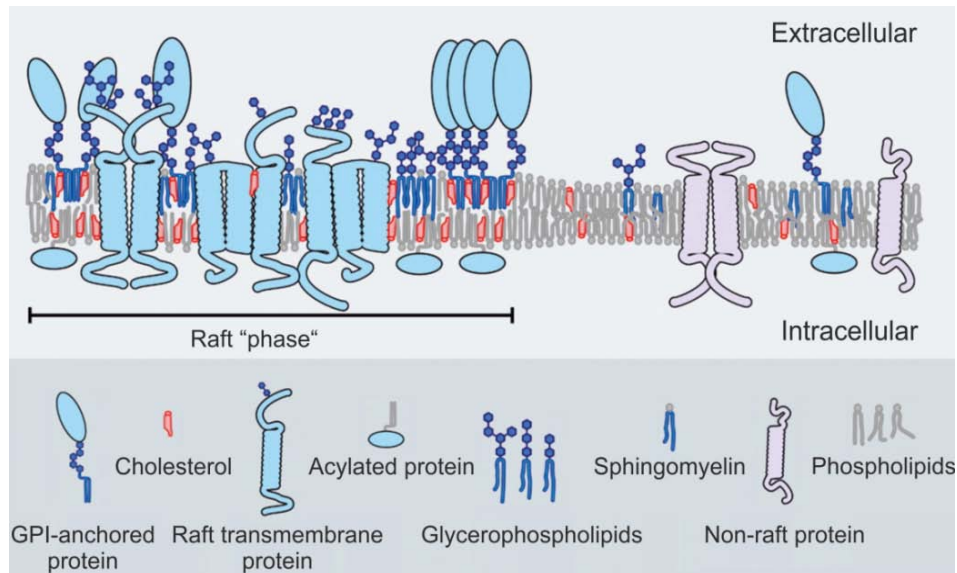
Figure 8.Membrane raft model. Model of the plasma membrane with an assembled membrane raft as proposed by Simons and Ikonen. Two decades later, the model has not disappeared but was controversly discussed(modified from Lingwood and Simons, 2010).

1.4.5Protein cluster theory

All the models shown so far help to understand the concept of the plasma membrane and its spatial lateral organization, but not all compartmentalization effects especially those involving proteins can be explained with these models.

In theory, for the picket fence model, all proteins with similar intracellular domains should be restricted in movement in the same manner and they should be located in the same membrane domains. Similarly, in the membrane raft model, since hydrophobic lipid-lipid or protein-lipid interactions are responsible for organization and arrangement, similar proteins should be arranged into the same domains. For both cases, experimental data proofed that the expected theories do not apply.

There are several membrane proteinsthat - even though their transmembrane domains are almost identical - are not found in the same membrane domains (Uhles et al., 2003; Zacharias et al., 2002).Furthermore, special motifs within the proteins can also be responsible for specific cluster formation and therefore for relocalizing proteins to distinct domains (Sieber et al., 2006).In the case of Syntaxin1A, a member of the SNARE complex, it was demonstrated how this protein forms protein clusters by protein-protein interactions. The size of a single cluster (Figure 9) is limited by the corresponding attraction forces that the proteins apply to each other.
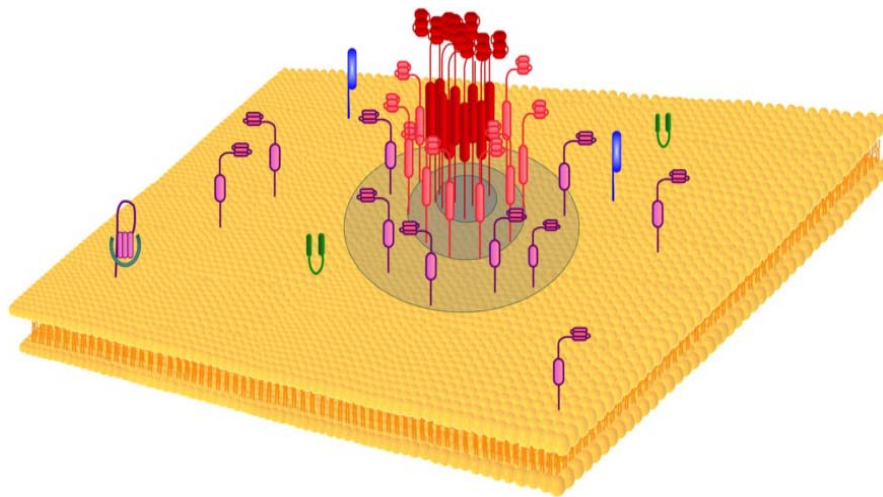
Figure 9.Model of a Syx1 cluster in the PM. Architecture of a cluster formed by Syntaxin1 on a lipid bilayer membrane.This model does not show the number of molecules per cluster but stresses a concentration gradient across the cluster(modified from Bar-On et al., 2012).

When the number of copies gets too high, the balance changes and repelling forces induce single proteins to be excluded from the protein cluster (Sieber et al., 2007).Dependency of clusters on a certain lipid composition (lipid-protein interaction) could also be shown; studies performed on SNARE proteins revealed that the formation of Syntaxin1A clusters are dependent of cholesterol and PIP2 (Lang et al., 2001, Chamberlain and Gould, 2002, Murray and Tamm, 2009).Additionally, a negative effect of lipid-protein interaction on

cluster formation was demonstrated in the presence of the plasma membrane lipid phosphatidylserine(Murray and Tamm, 2011).

The lipid raft hypothesis and its controversy were necessary for continuous intensive study of the membrane and especially the lipids. This controversy opened the door for new techniquesapplied on the analysis of native cell membranes (Simons and Gerl, 2010). By improving and developing microscopy methods and experimental setups many new insights weregained in this interesting field(Owen et al., 2012).

1.5 Enigmatic lipid domains – Difficulties and limitations

Experiments so far have shown that proteins and lipids areheterogeneouslydistributedalong the PM and might be arranged into nanodomains (Engelman, 2005).Important contributions to the current view on the architecture of the PM like the picket fence hypothesis or the protein cluster theory postulate proteins to be key players concerning the formation of such membrane domains.

But what about thelipid components of the PM?To date, only few lipids have been analyzed in detail in order to generally describe theorganization of potential lipid domains. According to the lipid raft theory, lipids are the major driving force for membrane organization. As already described (see *1.4.4membrane raft hypothesis*), a discussion has been carried out over the last two decades and there are numerous studies that either support or contradict this theory (Simons and Gerl, 2010). A final answer has not been foundpartially because of different interpretation of experimental results (e.g. detergent resistant fractions, see section *1.4.4*) but also due to technical limitations.Nevertheless, the following characteristics have been agreed on: Cholesterol and sphingomyelin can been detected in nanodomains with diameters of less than 20 nm (Sahl et al., 2010). Their dwell times in these domains

were calculated to be around 10 - 20 ms (Eggeling et al., 2009). The nanodomains themselves are short-lived as suggested by single molecule studies.

Protein domain studies outnumber the research on lipid nanostructures by quality and quantity.One reason for the imbalance isthat lipids are tedious biomolecules to deal with. Due to their hydrophobic characteristics, lipids require treatments for extraction and analysis that are laborious and tend to be more artifact-prone than for proteins. Furthermore, it is very challenging to tag lipids without altering their composition and physicochemical properties. These changesmight consequently influenceinteractions with their native environment. Additionally, lipids diffuse much faster than proteins across the PM making them difficult to image and they are present in higher number than proteins – for every single protein there are 50 lipids present (Jacobson et al., 2007).

1.5.1 Studying lipid nanodomains with single molecule approaches

As mentioned before, single molecule approaches helped to unravel some characteristics of lipid domains. One of the modern methods is fluorescence correlation spectroscopy (FCS) (He and Marguet, 2011). In FCS, a fluorescent particle is detected within a defined space and its fluctuation within this defined volume is measured. It is possible to deduce molecular aggregations of particles, calculate their flow rates or the rotational diffusion coefficients (Thompson et al., 2002). Nevertheless, in FCS the size of the volume that is used for measurements is a limiting factor. The latest FCS improvement regarding smaller sample volumes was made by including stimulated emission depletion microscopy (STED) resulting in STED-FCS (Eggeling et al., 2009; Mueller et al., 2011). Disadvantages of single molecule approaches include photobleaching effects that can lead to the incapacity of detecting very slowly moving or static objects. It is not possible to differentiate the already trapped molecules in a preexisting

domain from the ones that are immobilized by a domain that is formed when it is detected. In summary, it cannot be excluded that there are also small long lived lipid domains present in the PM of cells.

1.5.2 Lipid homeostasis

Lipids are not encoded in the genome, so cells have to take up these important constituents directly from nutrition and synthetize them de novo from precursors.Eukaryotic cells are able to synthesize thousands of different lipid molecules that are then incorporated into the multiple cellular membranes. This process involves the activity of enzymes that depending on their modification actions are responsible for the great lipid diversity. Additionally there are several, redundant, mechanisms to transport lipids from their site of synthesis to other cellular membranes. The different cellular compartments have also defined lipid compositions in order to function altogether with the corresponding proteins. Lipid transport has to be efficient for supplying the distinct membranes with their essential components. In general, the endoplasmic reticulum (ER) is the major site for lipid synthesis. Therefore intracellular lipid trafficking is necessary to maintain most other organelle membranes as they lack the capability to synthesize lipids de novo (van Meer et al., 2008). Because of their hydrophobic nature, most of the lipids cannot be transferred by free diffusion between compartments and must therefore rely on active mechanisms to facilitate transport. In principle, three basic mechanisms are applied (Blom et al., 2011).

First, membrane transport that involves the budding of vesicles from a donor membrane and subsequent fusion with an acceptor membrane is one form oflipid trafficking. Second, cells use cytosolic proteins for transferring lipids between compartments with the help of a hydrophobic lipid binding pocket that allowsbinding ofonly one lipid. Some lipid transfer proteins contain special binding domainsthat determine the donor and acceptor membranes, providing compartmental specificity for transfer (Blom et al., 2011). The third transport option is union of donor

and acceptormembranes in order to transferlipids via membrane contact sites. In vivo, combinations of these three mechanisms that act in parallel are responsible for lipid trafficking. In the present work, a lipid platform composed of PC is presented. Therefore the emphasis of this section is laid on the synthesis of this lipid in order to understand the importance within metabolic labeling process.

PC accounts for approximately 50 % of total cellular phospholipids and is the most abundant phospholipid in mammalian membranes (van Meer et al., 2008).PC is cylindrical in shape; as such, it is an important structural component that contributes to the integrity and function of membranes. It is essential for the formation and secretion of very low density lipoproteins by the liver, which is responsible for the delivery of hydrophobic cargo (cholesterol and energy in the form of fat) to other organs and it also plays a role in bile salt-mediated micelle formation in the intestinal lumen, which facilitates the absorption of lipid-soluble nutrients from the diet.

Mammalian cells are able to synthesize PC via two pathways: In the CDP-choline pathway choline entering the cell is rapidly phosphorylated by the choline kinase, converting it to phosphocholine (Figure 10). The second enzyme in this pathway, the CTP:phosphocholine cytidylyltransferase (CT) facilitates the conversion of phosphocholine to CDP-choline. The addition of the phosphocholine moiety to diacylglycerol completes the synthesis of PC. This reaction is catalyzed by CDP-choline:1,2-diacylgylcerol cholinephosphotransferase, or CPT, and occurs at the surface of the endoplasmic reticulum (Gibellini and Smith, 2010).
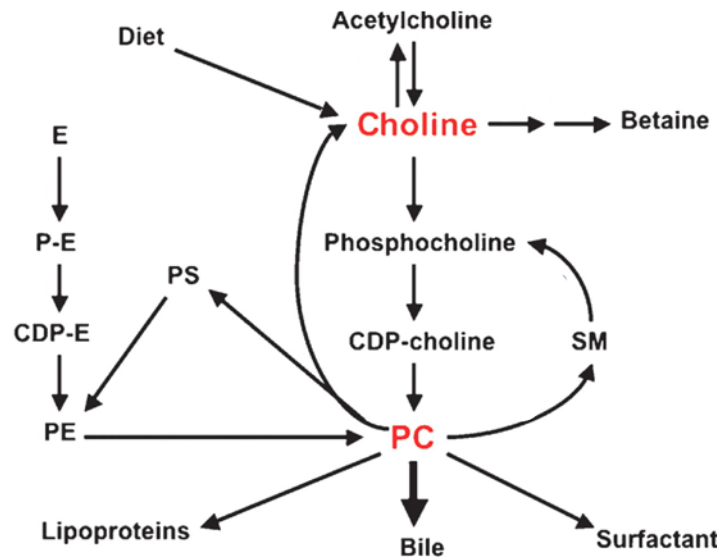
Figure 10: **Pathways involved in choline and PC homeostasis**

The figure shows the metabolic pathways of choline after uptake from diet in all nucleated cells (modified from Li and Vance, 2008).

The second synthesis pathway, also named phosphatidylethanolamine N-methyltransferase (PEMT) pathway primarily occurs in the liver. The hepatic cell has a high demand for PC due to the production and secretion of very low density lipoproteins and PC secretion into the bile, in addition to the normal cellular requirement for the synthesis of membranes. PEMT is an intrinsic membrane protein and active in the endoplasmic reticulum, where it performs three repeated methylation reactions converting phosphatidylethanolamine (PE) to PC. The methyl donor S-adenosylmethionine is required for each step of the reaction, generating three molecules of S-adenosylhomocysteine for each PC molecule produced. This mechanism contributes approximately 30% of PC produced in the liver, when choline supply is adequate to maintain PC synthesis through the CDP-choline pathway. However, when choline is limited in the diet, the PEMT pathway becomes critical.Once PC is synthetized it can be metabolized into sphingomyelin, a sphingolypid also found in mammalian cell membranes. The degradation of PC by a phospholipase results in lyso-PC (Pörn et al., 1993).

PC is part of all cellular membranes so it has to be transported from its site of synthesis (mainly the ER) to the different acceptor membranes.

The steroidogenic acute regulatory transfer (StAR) proteins belong to a superfamily of cytosolic proteins capable of binding specifically to lipids (and sterols) and are responsible for their transport (Alpy and Tomasetto, 2005). The main characteristic of the proteins is the START domain (~210 amino acids) which is a lipid binding pocket formed by α-helices. The family is composed of 15 proteins (in humans). An example of specific transfer proteins is StarD2 (also named phosphatidylcholine transfer-protein PC-TP) which binds to PC (Kanno et al., 2007).
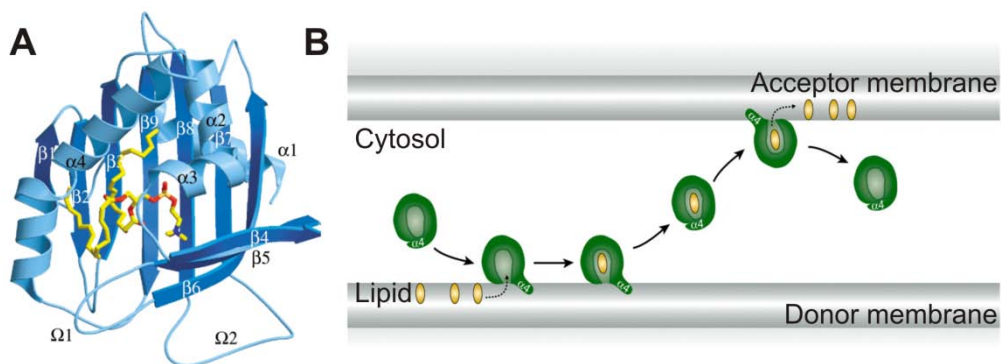
Figure 11.StarD2 and its mode of action. Ribbon diagram of StarD2 protein (A) in complex with PC (yellow stick model) and (B)its mode of action. START domain only proteins like StarD2 interacts with membranes through α-helix and opens the hydrophobic pocket for binding with the lipids. After complexing, the pocket closes and protein is able to target an acceptor membrane for delivery of the specific lipid (modified from Roderick et al., 2002; Alpy and Tomasetto, 2005).

1.5.3 Novel strategies for lipid labeling

An important achievement in recent years for studying lipids was the development of click chemistry. This "tailored chemistry" makes use of the cellular synthesis pathways to metabolically label defined lipids. This elegant method has the advantage that there are no major changes of the biochemical properties of the studied lipid. The bioincorporated label allows e.g. addition of a fluorescent probe that enables visualization of the studied lipid.

The practicability of the method was already mentioned a decade ago (Rostovtsev et al., 2002). For the labeling of PC(as first shown by Jao et

al., 2009), cells are fed with propargyl-choline which is then metabolized into propargyl-phosphatidylcholine (pPC). The newly synthetized pPC behaves as natural PC. The minor chemical difference is located on the choline head group where a small alkyne chain is present. This alkyne serves as anchorage site for cycloaddition of the azido-sulfo-Bodipy.
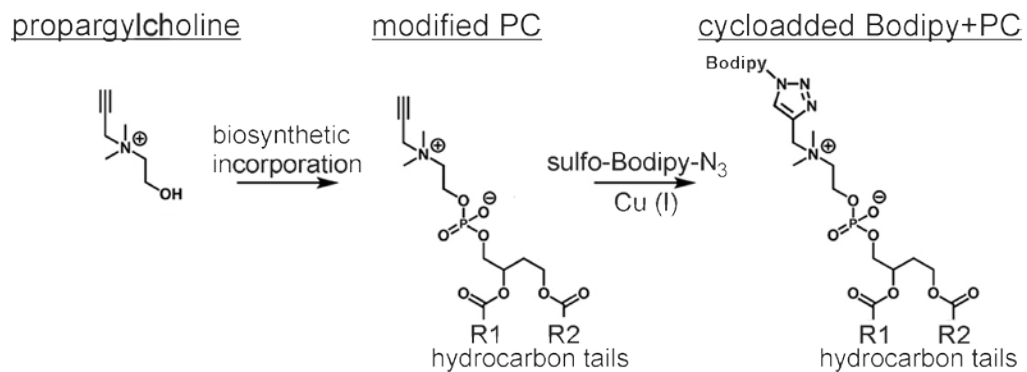
Figure 12.Cycloaddition of Bodipy to PC. First, propargyl-choline is supplied to cell medium that is biosynthetized into propargyl-phosphatidylcholine (pPC). Bodipy is then added to pPC by a Cu (I) dependent reaction of an alkyne group to an azide (modified from Jao et al., 2009).

1.6   Aims of the work

The aim of this work was to extend our understanding of phosphatidylcholine membraneorganization which is one of the major lipid components in plasma membranes. To this end, a novel approach for non-invasive lipid labeling was applied in combination with modern imaging techniques using cell free membrane preparations as biological samples.

One of the main aims was to test if click chemistry is a suitable tool for the analysis of lateral PC distribution and dynamics. The main question was, whether PC is laterally organized in a specific pattern within the plasma membrane. Any potential clusters or nanophases should then be characterized bydetermining thesize,calculating the phospholipid enrichment and measuring dynamics by attachment of fluorophores to metabolically labeled PC followed by the analysis of lateral PC distribution.

After characterization of potential nanophases, a description and analysis of their dynamics should be performed.

2. Materials and Methods

2.1 Materials

All chemicals, reagents and media used in the experiments described in this work are products of the German companies *Roth* (Karlsruhe), *Merck* (Darmstadt), *Fermentas* (St. Leon-Rot), *Sigma-Aldrich* (Hamburg), *Biochrom* (Berlin), *PAA Laboratories* (Cölben) and *Macherey-Nagel* (Düren), if not otherwise stated. All buffers and solutions were prepared using autoclaved distilled water.

2.1.1 Instruments and equipment

- Cell counting chamber (Neubaur 0640110, Paul Marienfeld GmbH)
- Confocal laser scanning microscope (Fluoview1000 (equipped with climate control), Olympus GmbH), supplemented with
  - 488 nm Laser (FVS-LDPSU, Olympus GmbH)
  - Control software (OlympusFluoview 3.0, Olympus GmbH)
  - Oil objective (UPLANSPO Oil 60x N.A 1,35, Olympus GmbH)
- DNA and protein concentration measurements (NanoDrop2000, Thermo Fisher Scientific)
- Epifluorescence microscope (Axio Observer D1, Carl Zeiss AG), supplemented with
  - CCD camera (12 Bit Sensicam QE, PCO AG)
  - Control software (Sensicam software, PCO AG)
  - Oil objective (Objective NA 1,4 x 100 Plan-Apochromat, Carl Zeiss AG)
  - Optical filter systems (DAPI, GFP, TRITC channel filters, AHF Analysetechnik AG)
  - Xenon lamp (XBO75 100.26B, LEJ GmbH)

- Extrusion device (Mini-Extruder, Avanti Polar Lipids Inc.)

- Extrusion membrane with defined pore size (Pore 50 nm (MB 19 mm 0.05 µm, cat. no.: 800308), Whatman, GE Healthcare Inc.)

- Filter support for extrusion membrane (Filter support (Drain disc 10 mm cat. no.: 8009220361) Whatman, GE Healthcare Incorporation)

- Freezing Container (5100 Cryo 1 °C Freezing Container "Mr. Frosty", Thermo Fisher Scientific)

- Gel documentation (DH-50, Biostep GmbH)

- Gel electrophoresis chambers, semi-dry blotting, power supply (Mini-Protean Tetra Electrophoresis, Semi-Dry Trans-blot transfer cell and Power Pac basic (and H), Bio-Rad Laboratories Incorporation)

- Membrane and gel scanning device (western blot) (Odyssey, Li-COR Incorporation)

- Microplate Reader (Infinite F200Pro, Tecan Trading AG)

- Microscope for cell culture (Eclipsets 1000, Nikon Instruments)

- PCR Thermocycler (T-Professional basic Thermocycler, Biometra GmbH)

- Sonifier (Sonoplus HD 2070, Bandelin Electronic GmbH)

- TIRF microscope (IX81-ZDC TIRF equipped with diverse magnification lenses (1x, 2x, 4x), Olympus GmbH), supplemented with
  - Control software (CellR, Olympus GmbH)
  - *EmCCD* camera (ImagEM C9100-13, 16 bit *EmCCD* camera, Hamamatsu Photonics Incorporation)
  - Filter set (U-MTIR488-HC, Olympus GmbH)
  - Laser beam (488nm Ag laser beam, Olympus GmbH)
  - Oil objective (Objective Apochromat NA 1,49 x 60, Olympus GmbH)

2.1.2 Buffers and solutions

Sonication buffer

120mM KGlu, 20mM KAc, 20mM HEPES-KOH, 10 mM EGTA; pH 7.2

KGlu buffer

120mM KGlu, 20mM KAc, 20mM HEPES-KOH, 10 mM EGTA; pH 7.2

Ringer Solution

130mM NaCl, 4mM KCl, 1mM $CaCl_2$, 1mM $MgCl_2$, 48mM D(+)Glucose, 10mM HEPES-NaOH; pH 7.4

PBS solution

2.7 mM KCl, 1.47 mM KH_2PO_4, 136 mM NaCl, 8.1 mM Na_2HPO_4; pH 7.3

PBS/BSA solution

2.7 mM KCl, 1.47 mM KH_2PO_4, 136 mM NaCl, 8.1 mM Na_2HPO_4; pH 7.3, 1% (w/v) BSA

PFA 16 % stock solution

Solution was kindly provided by Y. Okamura (preparation: 16% (w/v) paraformaldehyde in ddH_2O(solved at 65 °C adding NaOH drops);pH 7.2 after cool-down)

PFA 4% fixative

16% PFA stock solution diluted (1:4) in 1x PBS; pH 7.2

TMA-DPH solution

Saturated 1-(4-Trimethyl-ammoniophenyl)-6-phenyl-1,3,5-hexatriene p-toluolsulfonate (TMA-DPH; T204, Invitrogen, Carlsbad, USA) (1:3 in KGlu for membrane sheets or Ringer solution for whole cells)

Poly-L-lysine solution (20x Stock solution)

2 mg/ml poly-L-lysine-hydrobromide (Sigma, P1524) in ddH_2O

2.1.3 Cell culture media

PC12 standard medium

DMEM Glc 4.5 g/l with L-Gln with phenol red, supplemented with 1.6 mM L-Gln, 5% (v/v)inactivated FBS, 10% (v/v) horse serum, 1% (v/v) penicillin/streptomycin (penicillin 10.000 U/ml; streptomycin 10 mg/ml)

PC12 freeze medium

DMEM with phenol red, 20% (v/v) inactivated FBS, 10% (v/v) DMSO

PC12 delipidated medium

DMEM with phenol red, 10% (v/v) delipidated FBS, 1% (v/v)penicillin/streptomycin (penicillin 10.000 U/ml; streptomycin 10 mg/ml)

HepG2 standard medium

EMEM with phenol red, 10% (v/v) inactivated FBS, 1% (v/v)penicillin/streptomycin (penicillin 10.000 U/ml; streptomycin 10 mg/ml)

HepG2 delipidated medium

EMEM with phenol red, 10% (v/v) delipidated FBS, 1% (v/v) penicillin/streptomycin (penicillin 10.000 U/ml; streptomycin 10 mg/ml)

HepG2 high Ca^{2+} medium

Standard medium supplemented with 1.8 mM $CaCl_2$ and 20 μM ionomycin; pH 7.2

PC12 and HepG2 starving media

Standard medium without serum

2.1.3.1 Cell culture stock solutions

Fetal bovine serum (FBS)(cat. no.: S0615, Biochrom AG, Berlin, Germany)

Delipidated FBS

Delipidated FBS was kindly provided by C. Thiele and was prepared as already described (Camber and Knowles, 1976).

Horse serum (HS)(cat. no.: S9135, Biochrom AG)

2.1.4 Antibodies

Primary antibodies

Anti-His: mouse monoclonal IgG (cat. no.: sc-53073, Santa Cruz, USA). Antibody was used 1:200 for western blot analysis.

Anti-SNAP23: rabbit polyclonal IgG (cat. no.: 111203, SySy, Göttingen, Germany). Antibody was used 1:200 for colocalization experiments.

Anti-Syntaxin4: rabbit polyclonal IgG (cat. no.: 110043, SySy, Göttingen, Germany). Antibody was used 1:200 for colocalization experiments.

Secondary antibodies

Goat anti-mouse IRDye 800CW (cat. no.: 926-32210, Li-COR Biosciences, Nebraska, USA). Antibody was used 1:200.

Donkey anti-rabbit Alexa594 (cat. no.: A21207, Invitrogen). Antibody was used 1:200.

2.1.5 Reagents

Ionomycin solution (1000x stock)

20 mM ionomycin (cat. no.: Asc-116, Ascent Scientific, USA) in DMSO; pH 7.2

Protease inhibitors (25x)

Complete (mini), EDTA-free (cat. no.: 1836170, Roche). 1 tablet in 2 ml ddH$_2$O

PMSF

200mM phenylmethanesulfonylfluoride (cat. no.: 6367.2, Roth, Germany) in EtOH

Trypsin/EDTA

0.05% trypsin (cat. no.:L11-004, PAA Laboratories, Germany), 0.02% EDTA in 1x PBS

2.1.6 Click chemistry reagents (provided by C. Thiele)

Propargyl-choline-bromide

100mM propargyl-choline-bromide (Jao et al., 2009) in ddH$_2$O

TBTA

1mM TBTA (Tris[(1-benzyl-1H-1,2,3-triazol-4-yl)methyl]amine)(Sigma-Aldrich, cat. no.: 678937) in ddH$_2$O.

Cu (I) solution

1MTetrakis(acetonitrile)copper(I) tetrafluoroborate(cat. no.: 677892, Sigma-Aldrich) in acetonitrile.

Ascorbate solution

10 mM L-ascorbic acid (cat. no.: A4403, Sigma-Aldrich) in ddH$_2$O

Azido-sulfo-Bodipy

100mM azido-sulfo-Bodipy (i.e. 8-(5-Azidopentyl)-4,4-difluor-1,3,5,7-tetramethyl-4-bora-3a,4a-diaza-s-indacene-2,6-disulfonic acid disodium salt) (synthetized and kindly provided by Prof. Dr. C. Thiele) in ddH$_2$O

2.1.7 Mediumand buffers for bacteria

LB-medium

2% Lennox broth (w/v) in ddH_2O

LB-agar plates

2% Lennox broth (w/v), 2% agar (w/v) in ddH_2O

TYM-medium (complete medium)

2% (w/v) bacto trypton, 0.5 % (w/v) yeast extract, 0.1M NaCl, 10mM $MgSO_4$ in ddH_2O

SOB-medium

2 % w/v bacto trypton, 0.5 % w/v yeast extract, 0.01M NaCl, 10mM $MgSO_4$, 10mM $MgCl_2$ in ddH_2O, Mg^{2+}added after autoclaving;pH 7.0

SOC-medium

SOB-medium supplemented 20mM glucose.

Anhydrotetracycline (AHT) stock solution

10mg anhydrotetracycline (cat. no.: 2-0401-001, IBA technologies) in 10ml EtOH

TfB I-buffer

30mM KAc, 50mM $MnCl_2$, 100mM KCl, 10mM $CaCl_2$, 15% glycerol in ddH_2O

TfB II-buffer

10mM HEPES (pH 7.0), 75mM $CaCl_2$, 10mM KCl, 15% glycerol, in ddH_2O

2.1.8 Antibiotics

100µg/ml penicillin/streptomycin in corresponding medium

150µg/ml chloramphenicol in corresponding medium

100µg/ml ampicillin in corresponding medium

50µg/ml kanamycin in corresponding medium

2.1.9 Electrophoresisbuffers / SDS-Page

50x TAE buffer (DNA electrophoresis) Tris-acetate-EDTA

2M Tris, 50mM Na_2EDTA (pH 8.0), 5.71% (v/v) acetic acid (CH_3COOH) in ddH_2O

RIPA buffer

10mM Tris (pH 7,4), 150mM NaCl, 1mM EDTA, 1% (v/v) Triton X-100, 0.5% (v/v) DOC, 0.1% (w/v) SDS in ddH_2O

1mMPMSF,1x Complete[®] proteaseinhibitorsadded prior to lysis

SDS stock solution

10% SDS in ddH_2O(solved at 68 °C);pH 7.2

APS solution

10%ammoniumpersulfateinddH_2O

4 x Laemmli loading/sample buffer (SB)

250mM Tris (pH 6,8),30% (v/v) glycerol, 0.04% (v/v) bromphenol blue, 6% (v/v) SDS, in ddH_2O (20% ß-mercaptoethanol added freshly)

10x SDS transfer/running buffer

250mM Tris (pH 8,3), 1% (v/v) SDS, 2,5M glycine, in ddH_2O

12% SDS gel (2 gels)

Stacking gel: 3.05ml ddH_2O, 650 µl 30% acrylamid 0.8% bisacrylamid, 1.25ml 0.5 M Tris-HCl (pH 6.8), 50 µl 10% SDS

Resolving gel: 3.4ml ddH$_2$O, 4 ml 30% acrylamid 0.8% bisacrylamid, 2.5ml 1.5 M Tris-HCl (pH 8.8), 100µl 10% SDS

1x Transfer buffer (TB)

20%MeOH in 1x SDS buffer

10x TBS

100mM Tris, 1,5M NaCl in ddH$_2$O; pH 7.6

TBST

1% Tween-20 (v/v) in 1x TBS

Coomassie blue staining solution

0.25% Coomassie brilliant blue, 10% CH$_3$COOH,40% EtOHin ddH$_2$O

Coomassie blue destaining solution

20%MeOH, 10% CH$_3$COOH in ddH$_2$O

Gel drying solution

40% MeOH, 10% glycerol, 7.5% acetic acid in ddH$_2$O

Blocking buffer

LiCOR$^®$ blocking buffersolution (1:1) in 1x TBS

2.1.10 Protein purification solutions

Sonication buffer

50mM Tris (pH 8), 300mM NaCl, 1% (v/v) Triton-X 100, 1x Complete$^®$ EDTA-free, 1mM PMSF, 100µg/µl lysozyme in ddH$_2$O

Binding buffer (BB)

20mM Tris (pH 8), 150mM NaCl, 1x Complete$^®$ EDTA-free, 1mM PMSF, Ni-NTA beads (Protino$^®$ cat. no. 745400.25, Macherey&Nagel, used 1:10) inddH$_2$O

Elution buffer

20mM, Tris (pH 8), 150mM NaCl, 1x Complete$^®$ EDTA-free, 1mM PMSF, 20mM (40mM; 75mM; 150mM; 300mM) imidazole in ddH$_2$O

2.1.11 *E.coli* strains

E. coli XL10-Gold ultracompetent cells (Stratagene cat.No.:200315) were used for cloning of the vector pASK-IBA 43+ containing the specific StarD protein for purification of plasmids when required.
E. coli BL-21 (DE3)pLysS (Promega, cat No.: C6020-03)were used for overexpression and purification

2.1.12 Kits (cloning/ purification of DNA/ protein quantification)

NucleoSpin Extract II (cat. no.: 740609), NucleoSpin Plasmid (cat. no.: 740588), NucleoBond PC 500 (cat. no.: 740574), NucleoBond Xtra Maxi Plus (cat. no.: 740416). Both Nucleospin kits (MACHEREY-NAGEL GmbH & Co. KG, Düren)

Zero Blunt TOPO$^®$ PCR Cloning Kit (cat. no.: K2800-20, Life Technologies GmbH, Darmstadt).

BCA protein assay Reagent (cat. no.: 23225, Thermo Scientific Pierce Protein Biology Products, Rockford, USA)

2.1.13 Cell lines

HepG2

HepG2 cells are derived from ahuman liver tumor (HepG2 cells, *homo sapiens*, ATCC: HB-8065).The cell line was kindly provided by Prof. Dr.

Famulok. The identity of the cells was verified applying geneticin (G-418) and checking for trypsin resistance and morphology. HepG2 cells were splitted every 3 days when confluency of the flask was about 90%. Splitting was performed always 1:3 and for longterm storage, 2.5×10^6 cells were frozen in cryovials.

PC12

Cells originate from pheochromocytoma from the rat adrenal gland (PC12 cells, clone 251, *rattus norvegicus*, ATCC: CRL-1721, Heumann et al., 1983).This cell line was splitted every 3-4 days when confluency of the flask was about 80%. Splitting was performed always 1:3 and for longterm storage, 2×10^6 cells were frozen in cryovials.

2.1.14 DNA constructs

pASK-IBA43+StarD2 was cloned from a construct originally prepared by E. Guhr and was described in her Bachelor thesis (Guhr, 2005). The construct was kindly provided by Prof. Dr. C. Thiele.

2.2   Methods

2.2.1 Preparation of chemocompetent E. coli

In principle any *E. coli* strain can be transformed into chemocompetent bacteria. Therefore this protocol can be generally applied. First, *E.coli*strain is inoculated on a LB_0 agar plate (6 cm petri dish) and incubated ON at 37°C.From the LB_0 agar plate, 100 ml TYM medium were inoculated with a single colony and incubated overnight at 37 °C. The next morning, bacterial OD_{600} was measured and diluted to $OD_{600} = 0.1$ in 500 ml TYM medium. The flask was incubated at 37 °C and shaken (160 rpm).

When $OD_{600} = 0.6$ was reached, the bacteria suspension was centrifuged (at 4 °C) at 4000 rpm for 8 min. The supernatant was then

discarded and the pellet resuspended in 100 ml ice-cold Tfb I solution. Immediately, the suspension was centrifuged again at 4000 rpm at 4 °C for 8 min. The supernatant was discarded and the pellet resuspended in 20 ml Tfb II solution and triturated. The solution was then dispersed in 200 µl aliquots and immediately frozen and stored at -80 °C.

2.2.2 Cloning of StarD2

All cloning procedures were performed according to standard PCR and microbiological protocols as described by Sambrook and Rusell (Sambrook and Rusell, 2006). The oligonucleotides were ordered from MWG Operon (Obersberg, Germany) and sequencing was performed by GATC (Konstanz, Germany).

The proteins of interest were already cloned in the vector pN3HA (kanamycin resistance, prepared by C. Thiele, 2005). This vector contained the wildtype StarD2 protein. StarD2 sequence specific primers(Table 2) were used for Gateway-cloning into the TOPO® vector prior to final insertion into pASK-IBA43+ vector for overexpression in bacteria. The vector was purchased from IBA technologies (cat. no.: 2-1443-000). Expression of the final vector results in a double tagged protein: an N-terminal 6x*Histidine-tag*and aC-terminal *strep-tag*.

Table 2. Primerused for cloningStarD2 into pASK-IBA43+ vector

D2_FWD	GCGGGG GAATTC ATGGAGCTGGCCGCCGGAAAC
D2_REV	GCGGGG GGATCCGGTTTTCTTGAGGTAGTTCTG

The constructs were amplified when required in *E. coli* bacterial lines DH5a, Top10, XL1-blue or XL10-gold. DNA purification was performed with kits as described by the manufacturer.

2.2.3 Protein purification of StarD2

StarD2 (PC-TP) was cloned into pASK-IBA-43+ (IBA Technologies). Plasmids were transformedinto *E. coli* BL21(DE3), and protein expression was induced by addition of 200µg AHT (when OD_{600} = 0.6) to 1L LB followed by 8h of shaking (250 rpm) at 18 °C.Bacteria were pelleted by centrifugation, lysed bysonication in sonication buffer and centrifuged (4200rpmfor 20min at 4 °C). His-tagged proteins contained in the bacterial supernatants wereadsorbed to nickel beads (preincubated for 45min with sonication buffer, then centrifuged 500 xg for 1min) within a falcon tube. After a total incubation time of 4 hwith the beads (at 4 °C) on a rotating device, the proteins were washed in BB (flowthrough sample was taken for WB analysis)and elutedusing a stepped imidazole gradient (2x 20mM in 5ml BB and 1x 300mM in 5ml EB). For desalting and exchange of buffers, solutions containing StarD2were appliedto a PD10Sephadex®G25 column (GE Healthcare). The column was previously equilibrated withbuffer (e.g. KGlu buffer when working on membrane sheets; PBS was the elution buffer when the proteins should be used on liposomal assays).After purification, *his*-tagged recombinantproteins yielded single bands as assessed by SDS-PAGEfollowed by Coomassie brilliant blue staining. Protein concentrationswere determined according to their molar extinctioncoefficients at 280nm, which were calculated based on aminoacid sequences (www.expasy.org).

2.2.4 BCA test

The BCA test was purchased as a kit and it was prepared according to manufacturer's orders and the absorbance at 592 nm was measured in a 96-well in a microplate reader. The concentration was then calculated using the standard BSA as described by the manufacturer.

2.2.5 SDS-PAGE and Western blot analysis

Unless otherwise stated, 1 x10^7 cells were centrifuged (1000 rpm, 3 min) and the pellet was washed twice with 1x PBS. Then, the pellet was resuspended in 80 µl RIPA buffer and kept on ice for 30 min. After lysis, the sample was centrifuged at 4 °C at 750 rpm and the supernatant was transferred into a new tube. Both samples were then frozen in liquid nitrogen and stored at -80 °C until needed for the corresponding experiment. In the case of protein purification by bacterial overexpression the samples were taken in every step of the purification protocol for quality control and optimization. For cells, 30 µg samples were applied in lanes, for protein purification the same volume was taken in order to provide a possibility for later comparison of amounts in gels. The samples were pelleted and resuspended in 50µl 1xSB and incubated at 99 °C for 5min. SDS-PAGE and semi-dry blotting were performed as already described (Kyhse-Andersen, 1984). SDS-PAGE was performed on 12 % acrylamide gels. After semi-dry blotting the nitrocellulose membrane was blocked with the LiCOR$^®$ buffer and stained with the corresponding Ab for the proteins of interest. Detection of the fluorescent secondary Ab (IRDye 800CW) was performed on the Odyssey imaging system.

2.2.6 Coating of glass coverslips with poly-L-lysine

For all experiments with microscopy analysis, cells were seeded on coverslips (radius 25mm, degree 0, cat.No.: 0110650, Marienfeld, Germany). The glass cover slips were first shaken carefully for 1h in 1M HCl, then washed 3x with ddH$_2$O. Afterwards, they were shaken gently for 1hwith 1M NaOH. The coverslips were washed again 3x with ddH$_2$O. Finally, they wereshaken for 2h in EtOH (absolute) and after discarding the EtOH, the cover slips were autoclaved.

The cover slips were dispersed in 6-well plates and coated with 500µl of a 1x poly-L-lysinesolution. After 20min of incubation, the solution was

aspirated and the coverslips were washed 2x with ddH$_2$O. The water was discarded and the cover slips dried for 2h under the sterile hood. The 6-wells were stored at 4 °C until needed for the experiments.

2.2.7 Cell Culture

The cell lines mentioned before were cultivated under sterile conditions and kept in standard cell culture vessels (Sarstedt, Nürnbrecht and Labomedic, Bonn, Germany).

Thawing, splitting, seeding and freezing of cells

The first passage was thawing cells from liquid nitrogen. The cryovial was allowed to thaw in a water bath at 37 °C for 3min and then the cells were quickly transferred into a 25cm^2 cell culture flask and cultivated overnight in 10ml cell specific medium. The next morning, the medium was changed. Once the cells reach a high confluence, the first splitting was performed.

Both cell lines were maintained in 75cm^2 tissue culture flasks containing 25ml of cell specific medium (see cell culture media and buffers). The cells were incubated at 37 °C, 10% CO$_2$ and 90% relative humidity in sterile incubators and allowed to grow 3-4 days to attain a confluence before splitting into fresh flasks.

Prior to splitting, the cells were washed with PBS and then detached from the vessel using 2ml of trypsin/EDTA. After 5min incubation at 37 °C, trypsin was inactivated by adding 10ml cell specific medium and the suspended cells were then centrifuged in a 50ml falcon tube at 1000rpm for 5min at RT. The supernatant was then removed and the cells were resuspended and triturated 10x in 10ml medium for either continuous cell culture (split 1:3) in a fresh flask or -using a dilutionof 1:10 in PBS- counted in a Neubaur counting chamber in order to use a defined cell number for the corresponding experiment. When cells were

seeded on poly-L-lysine coated cover slips, usually 500,000 cells per coverslip were used, unless it is otherwise stated. The seeded cells were kept for 20min at 37 °C and 5% CO_2 in the incubator and after this adhesion time, 2ml cell specific medium was given into each well. For cycloaddition experiments, cells were washed after 4h with warm 1x PBS and cell specific delipidated medium supplemented with 0.5mM propargyl-choline is added. The 6-wells were then further kept in the incubator for 8h. Only cells in the passage number 4-20 were used and a feeding time of 8h corresponded to overnight feeding.

For long-term storage of cells, $2x10^6$ cells of each cell line were frozen using 1ml of the corresponding freeze medium. The cells were keptin cryovials in a gradient freezing chamber filled with isopropanol for 24h and then changed to a liquid nitrogen container.

2.2.8 Preparation of membrane sheets

Membrane sheets allow in a cell-freesystem for visualization and analysis of lipids and proteins under native conditions. In order to prepare membrane sheets, adherent cells are "unroofed". This can be achieved by mechanical stress (Fujimoto et al., 1991) sliding glass cover slips or even easier by a sonication pulse (Lang, 2003). After applying a single ultrasonic pulse on adherent cells, only the attached basal plasma membrane stays on poly-L-lysine coated thin glass cover slips (Figure 13). The prepared membrane sheets are biochemically still active and are accessible for immunofluorescent staining of proteins by antibodies or for analysis of exocytotic processes (Avery et al., 2000). This method has gained popularity in the last decade due to its powerful advantage of having a natural environment for proteins or lipids of interest that are present in the plasma membrane.
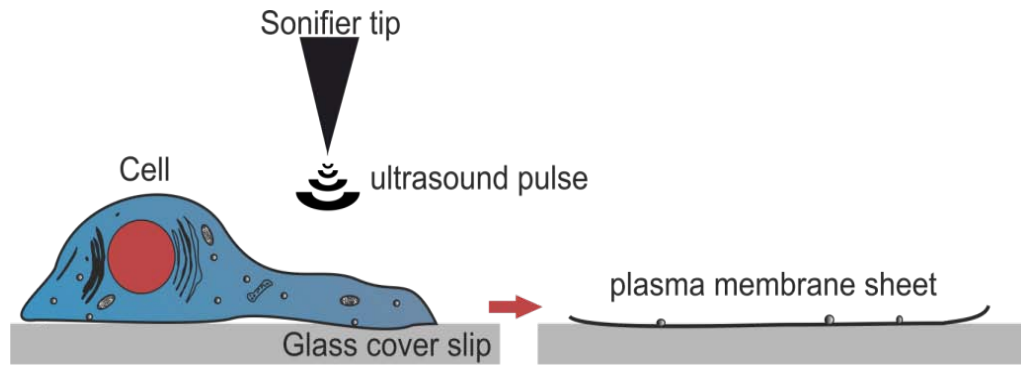
Figure 13.Preparation of membrane sheets.

Adherent cells are cultivated on cover slip. After sonication, the cells are "unroofed" and the remnant membrane is the so-called *membrane sheet*.

In the present work, membrane sheets were prepared from cells incubated overnight seeded on PLL-coated cover slips. First of all, every single cover slip was submerged in 20 ml ice cold sonication buffer. The sonicator tip was brought closer (and also submerged) to the coverslip with the cells facing towards the tip (distance ~0.5 cm). Then, an ultrasonic impulse was applied (0.1 s) with the optimized specific strength for the corresponding cell line. Normally, a star-shape is visible, meaning that within the branched regions the cells have been unroofed, so one can find native plasma membrane sheets attached to the cover slip surface. Membrane sheets are still biochemically active and accessible for e.g. immunohistochemical staining. The sheets can be used directly in native form or fixed for 0.5 h – 1 h in 4% PFA in 1x PBS and then quenched with 50 mM NH_4Cl.

2.2.9 Immunostaining of membrane sheets

Immunostaining of membrane sheets was performed as already described (Lang et al., 2001). Membrane sheets were fixed with 4% PFA and afterwards washed in 1x PBS. Then, 50mM NH_4Cl in 1x PBS was added in order to quench the fixative for 20min. The samples were then incubated with 150µl primary antibodies (see section *Primary antibodies*) upside down on parafilm for 45min at RT in a moist chamber and washed three times in 1x PBS for 5 min each, followed by 45min incubation with the respective secondary antibody (150µl each sample) conjugated to a fluorescent dye (see section *Secondary antibodies*).

2.2.10 Incubation of membrane sheets with lipid transfer protein StarD2

After protein purification and quantification via BCA test (see below), the protein was used for incubating membrane sheets. The amount of protein used in experiments varied depending on the purification values. For quality reasons low amounts were used for initial experiments on native membranes since experience in preliminary experiments showed that the lipid transfer proteins have a very high efficiency rate and effect on membranes. For StarD2, 100nMor 250nM working concentrationswere used.

2.2.11 Increase of intracellular calcium levels inside cells

As mentioned before cells were seeded on PLL-coated cover slips and incubated ON. The next morning, the medium was discarded and cells were washed twice with 2ml PBS. Then, the cell specific medium pH 7.2 supplemented with 20mM ionomycin (+10mM EGTA in control conditions) was added to the cells. The plate was incubated at 37 °Cfor 5min, afterwards the medium was discarded and 2ml 1xPBS was added to the cells. The cells were then immediately used for preparation of membrane sheets and click reaction.

2.2.12 Cycloaddition of dyes

The cycloaddition reaction was performed on fixed cells as well as either fixed or native membrane sheets. In a separate FRAP condition;sheets were also fixedafter performing the cycloaddition reaction. Priorto preparation of membrane sheets, a click reaction mix was prepared (625µM TBTA, 500µM ascorbate, 500µM Cu(I) and 100µM azido-sulfo-Bodipy in 1x PBS)and samples were incubated for 30min at RT within a moisture chamber. The coverslips were then washed twice in 1x PBS. For STED microscopy, azido-coupled Atto647N (AD647N-101, ATTO-tec, Siegen, Germany) was employed (instead of the azido-sulfo-bodipy) using the click-iT cell reaction buffer kit (C10269, Invitrogen).

2.2.13 Thin layer chromatography

50,000 HepG2 cells per condition were harvested from 6-wells by scraping, followed by washing in 1x PBS, centrifugation and the cell pellet was frozen in liquid nitrogen. For lipid extraction, the pellet was resuspended in 1ml (1:3 chloroform/methanol), vigorously shaken and centrifuged (4500rpm for 5min at RT). The supernatant was then mixed with 400µl ddH$_2$O and 600µl chloroform. After phase separation the upper phase was removed and the remaining lower organic phase was evaporated. Lipids were dissolved and incubated for 3h at 40 °C in cycloaddition mix containing 2.3mM Cu (I) tetrafluoroborate, 81µM hydroxyazidocoumarin(Thiele et al., 2012)in EtOH. After the cycloaddition reaction, samples were loaded onto TLC plates (without fluorescent indicator). TLC was performed first in CHCl$_3$/MeOH/H$_2$O/HOAc (65:25:4:1) followed by running in hexane/ethylacetate (1:1) for full plate distance. Finally, the plate was dried and exposed to 3% Hueing base in hexane. Fluorescent-labeled lipids were detected by excitation at 420nm and detection at 494 nm. Images were quantified by using the gel-pro software.

2.2.14Microscopy methods

2.2.14.1 Epifluorescence microscopy

Epifluorescence microscopy is the most common method for visualizing biomolecules of interest that have been tagged with a fluorophore either by biomolecular methods (cloning of proteins and fusion to EGFP), by immunofluorescent labeling (antibodies raised against a certain protein that again are tagged by secondary antibodies attached to a marker e.g. Cy3, Alexa594®), or by chemical attachment of a fluorophore (e.g. Bodipy) as in the case of click chemistry (see section below). In epifluorescence the basic setup is a light source (normally a xenon lamp) followed by a filter system that excites distinct fluorescent probes with different excitation ranges, the optics system, and a CCD camera that captures images from the sample. Epifluorescence microscopy can be used when imaging of cytosolic tagged biomolecules is necessary rather than exact analysis of membranes. The disadvantage is the strong out of focus fluorescence signals that are emitted and not filtered in the setup.

For this work epifluorescence microscopy was performed on native plasma membrane sheets with a Zeiss Axio Observer D1 fluorescence microscope. A majority of the experiments were performed with membrane sheet preparations. Even though *in vivo*conditions are obviously not present anymore, the preparations are perfect for analysis of the native plasma membranes. In order to visualize the integrity of the plasma membrane, staining by TMA-DPH was used. TMA-DPH is only able to emit fluorescence when it encounters a lipid environment as in the plasma membrane. This fluorescent intercalating membrane marker was detected in the DAPI channel of the microscope. From now on, the GFP channel is denominated as the Bodipy channel from which the signal of cycloadded Bodipy to the PC was detected. The TRITC channel was used for additional staining by Ab AlexaFluor594 for colocalization analysis with proteins. The illuminating time used for

DAPI and Bodipy was 400 ms and for TRITC 1 s, unless stated otherwise.

Raw data images were analyzed with the program imageJ (Schneider et al., 2012). First, images taken in different channels were aligned in the red and green channels. For lateral alignment tetraspeck beads were used as reference. Then, for calculation of the correlation coefficient the imageJ plugin colocalization indicesanalysis (Nakamura et al., 2007; Sieber et al., 2007) was used in a square ROI (150 x 150 pixel). Resulting correlation coefficientvalues from membrane sheets per independent experiment were averaged. For every individual experiment at least 15 spots per membrane sheet from 15 membrane sheets were analyzed.

For spot over background analysis, round shaped 7 x7 pixel ROIs were centered randomlyover individual spots in the Bodipy channel and the same 7 x7 pixel ROIs was placed on the uniform layer of the sheet next to the spot. These spots were then transferred to the aligned red channel. A background valuewas taken fromproximity to the sheet and the value was subtracted from mean intensity values of the spots in both channels and the ratio between spot and background was finally calculated for at least 15 spots per sheet and 15 sheets in one individual experiment.

Visualization of the movement of PC platforms was additionally incorporated in this work. The experiment was designed together with E. Merklinger who then performed the experiment and G. Schloetel assisted on the analysis.

2.2.14.2 Total internal reflection (TIRF) microscopy

TIRF microscopy is used to analyze biomolecules present in the basal membrane of cells. In a TIRF setup, a laser beam is applied on a cell in

a defined critical angle in order to create an evanescent field of excitation light that is around 100 nm. In this case, only fluorescence within this depth can be detected (Steyer and Almers, 2001). The excitation in this range enables the detailed visualization of the plasma membrane of living cells that are in close proximity of the glass cover slip that they are attached to (Figure 14). Such a specialized visualization improves the signal to noise ratio diminishing the undesirable out of focus fluorescence that might be created by fluorescence coming from inner compartments of cells e.g. Golgi apparatus or endoplasmic reticulum.
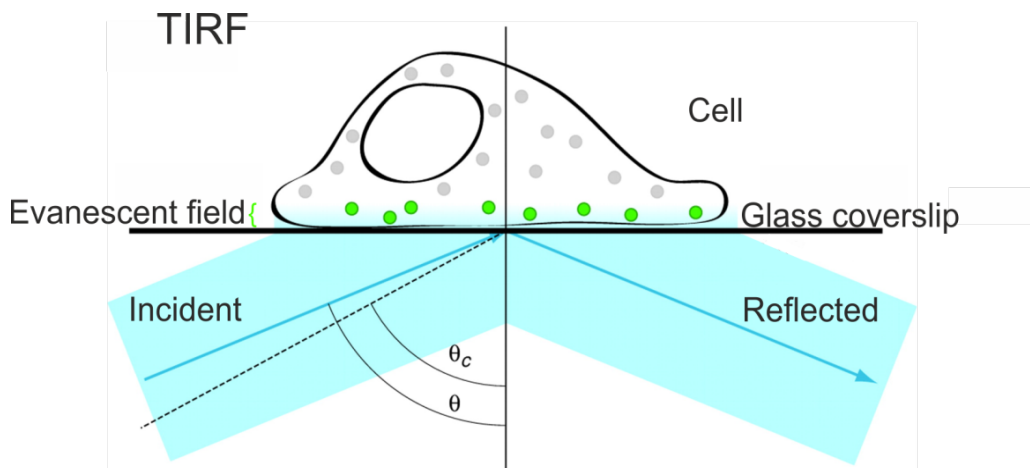

Figure 14.Physical principle of TIRF microscopy.
The excitation beam hits the coverslip at incident angle θ which is greater than the critical angle θc (dashed line). The excitation beam is reflected off the coverslip and an evanescent field is generated in the cell side (modified from Mattheyses et al., 2010).

Total internal reflection fluorescence (TIRF) microscopy was performed as part of this work as described previously (Schreiber et al., 2012). Cells were fixed for 30-45 min at RT with 4% PFA in 1x PBS, followed by quenching with 50mM NH_4Cl in 1x PBS. Then Bodipy was cycloadded as previously described. Fixed cells (minimum 15 cells are imaged for every single experimental day) were imaged at RT in Ringer solution (containing TMA-DPH). The TIRF microscope components are described in section *2.1.1 Instruments and equipment*. The combination of magnifying lenses, objective and the *EmCCD* camera ended in a

pixel size of 83.3nm. Images were acquired with CellR Olympus software and exported into TIFF format for further processing in imageJ.

2.2.14.3 High resolution microscopy: stimulated emission depletion (STED)

STED microscopy enables to break the resolution limits of conventional microscopy. It is based on confocal laser scanning microscopy with the difference that two laser beams are used in this method. One laser excites the probe while another overlaps with a donut shape over the excitation in order to reduce the region of interest by simply depleting the outcoming signal to a defined region in nm size (Figure 15). The signal is then detected and a computer generated image is obtained. A STED setup is capable of a resolution of 15 nm/pixel. The greatest advantage of having a better resolution is the possibility to accurately calculate the size of clusters that might be found on cellular membranes in order to e.g. calculate the number of biomolecules that are present in nanophases.
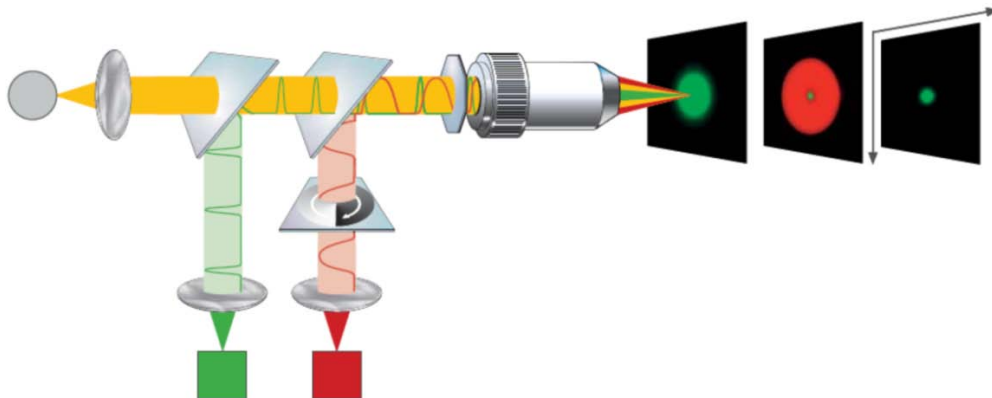
Figure 15.Simplified excitation and detection path of a STED microscope.

The excitation laser (green) and the STED depletion beam (red) are focused into the specimen to yield a diffraction limited excitation spot and a donut shaped STED point spread function (PSF), respectively. A helical phase plate in the STED beam path generates the donut shape of the STED-PSF. Fluorescence (yellow) is recorded by a point detector (modified from Hell and Wichmann, 1994).

For the STED microscopy applied in the present work a Leica TCS SP5 STED microscope equipped with a 100x 1.4 NA HCX PL APO CS oil objective as previously described (Denker et al., 2011) was used. These experiments were performed at the European Neuroscience Institute in the Laboratory of S. O. Rizzoliin Göttingen, Germany. S. Saka performed 2 experimental days.

For spot size analysis, a 150 x 150 pixel ROIwas randomly chosen. Linescans with a size of 3 pixels wide and 30 pixels long were placed on the center of clusters available within the ROI. By obtaining intensity profiles of individual spots the values were then fitted using a Gaussian function (OriginPro 8.0, OriginLab Corporation). The size of the full width at half maximum (FWHM) was determined and averaged of at least 200 spots on 10 membrane sheets for each individual experimental day.

For spot over homogenous layer intensity ratio analysis, the same 150x150 pixel ROIs as in the spot size analysis were used. A circular region of 7x7 pixels was laid over every single spot and over the closest surrounding of the spot. Additionally, a background measurement was performed on the original size images (1024x1024 pixel) for later subtraction from the measured circular ROI and the homogenous layer. The background corrected values were then divided for calculation of the spot over layer intensity ratio and averaged.

2.2.14.4 Confocal laser scanning microscopy (CLSM) and fluorescence recovery after photobleaching (FRAP)

FRAP is a method commonly used for studying dynamics of proteins that are overexpressed and attached to a fluorophore reporter molecule such as EGFP. The experiment is performed with a confocal laser scanning microscope. Excitation is provided by a laser with a defined wavelength for the corresponding fluorescent probe and the detection is done by calculation of the fluorescence signals that arrive at the

photomultiplier detector. FRAP can be observed when applying high intensities of excitation light. The increase in energy of the excitation laser beam leads to bleaching in a previously defined region of interest (ROI) due to chemical modification of the fluorophore caused by the electrons excited during fluorescence. The defined ROI is measured continuously afterwards in order to quantify the recovery rate of fluorescent signals. A recovery is seen due to diffusion of the fluorescent biomolecule from unbleached regions of the PM into the ROI.

In this work, FRAP was performed at RT and confocal laser scanning microscopy (CLSM)in an environment control chamber at 37°C using an OlympusFluoview1000 laser scanning microscope as described previously (Zilly et al., 2011). Pixel size was adjusted to 69nm, dwell time to 20µs/pixel and the image size to 200x200 pixels. Bleaching was performed in a 30x30 pixel ROI using the 488nm laser at full intensity. First, the pre-bleach frame was recorded, then the sample was bleached immediately followed by the post-bleach recording and then another recording 60 sec after the pre-bleach frame. In control experiments for bleaching of whole membrane sheets, an adequate size was chosen in order to keep the settings for the bleach protocol as just mentioned and secondly a size was chosen that allows acquisition of whole membrane sheets. Single measurements were made to show the rapid recovery. In that case the pre-bleach phase is 3 frames acquired at 1 Hz, bleach phase is 1 frame at 1 Hz and post-bleach 6 frames at 1 Hz.

For analysis, spot over homogenous layer analysis was performed within the bleach region as described above. Only spots showing at least 50% local increase before bleaching are included in further calculations.

3.   Results

PC is the most abundant phospholipid within the plasma membrane of mammalian cells and yeast. It has been considered as a passive component and classified as cylindrically shaped constituent of the PM having less influence in the curvature than other conical (e.g. PE) or inverted conical (e.g. SM) classified lipids (Simons and Sampaio, 2011).Yet, there is no clear picture of the organization of PC within the plasma membrane. To clarify this question, a wide range of microscopy methods were combined with click-chemistry to study this major component of the PM. Cycloaddition of azido-sulfo-Bodipy has already been demonstrated to be a useful tool to label PC in whole cells (Jao et al., 2009). These early experiments showed a labeling of the multiple cellular membranes. In the present work, metabolic PC-labeling/click-chemistry was applied to study nano-anatomical aspects of PC organization and dynamics not onlyfor whole cells but also in native membrane sheets.

3.1 Labeling with Bodipy and detection of pPC in the plasma membrane of mammalian cells

HepG2 and PC12 cells were seeded and fed ON with propargyl-choline and then fixed with 4% PFA. Fixation with 4 % PFA in general leads also to permeabilization of cells, so also intracellular pPC will be labeled with the fluorophore and can be potentially visualized. After cycloaddition of azido-sulfo-Bodipy to pPC, the samples are imaged with a TIRF microscope setup. Initially epifluorescence shows a bright signal viewed in HepG2 and PC12 cellsdemonstrating the high amount of pPC in all cellular membranes. Then, by applying TIRF microscopy,selectivelythe basal plasma membrane of cellswas observed.

As expected, pPC formed a uniform background but also a major number of remarkably clear visible spots were seen (Figure 16).

The presence of pPC in spots within the plasma membrane gave a first hint about a lateral organization of the pPC.
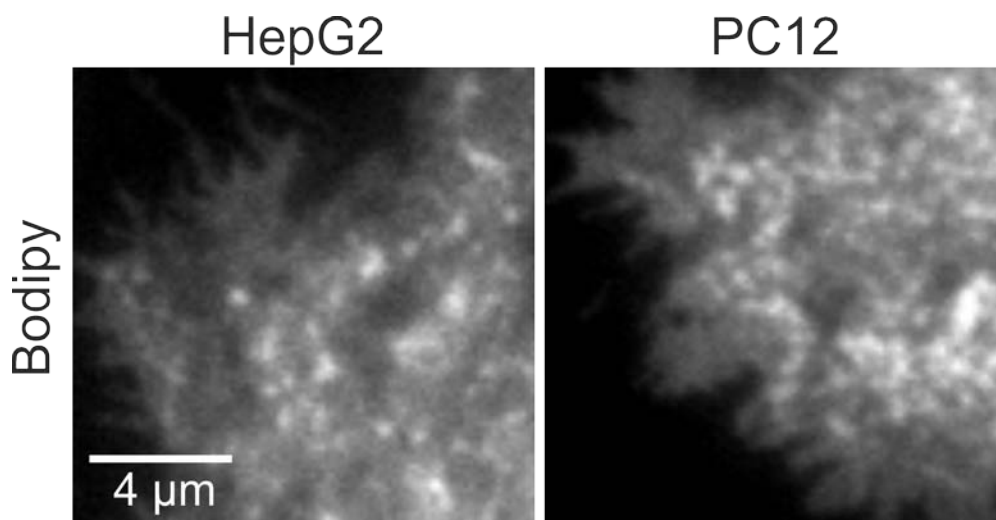

Figure 16. PC forms spots in the plasma membrane of whole cells.

HepG2 and PC12 cells were fed with propargyl-choline ON and fixed in 4% PFA. After cycloaddition, imaging was performed in a TIRF microscopy setup having first visualized the target cells in epifluorescence mode (not shown) and then switching to TIRF-modus to visualize the basal plasma membrane of cells. The left panel showsBodipy signal of a representative HepG2 celland right panel a PC12 cell in TIRF-modus.

3.2 Labeling of pPC on membrane sheets shows spots

Again, cells were seeded on PLL-coated glass coverslips and fed ON with propargyl-choline. Native membrane sheets were prepared from two different cell lines (HepG2 and PC12) by applying a short ultrasonic pulse to the cells (see section*2.2.8Preparation of membrane sheets*). Then, click-chemistry was applied. Membrane sheet preparations help to visualize the pPC spots within the native plasma membrane with a better signal to noise ratio due to the lack of the remaining cell body. In order to visualize the membrane sheets and check their integrity a TMA-DPH staining is required.TMA-DPH is an intercalating agent and

its fluorescence increases in the presence of lipids. This staining helps to visualize and select only those membranes that have not been completely ruptured by the sonication process. The results are shown in figure 17.

Click reaction control was performed by preparing cells that were not fed with propargyl-choline. After click reaction, these cells or their membrane sheet preparations did not show a fluorescence signal (data not shown) in the Bodipy channel.
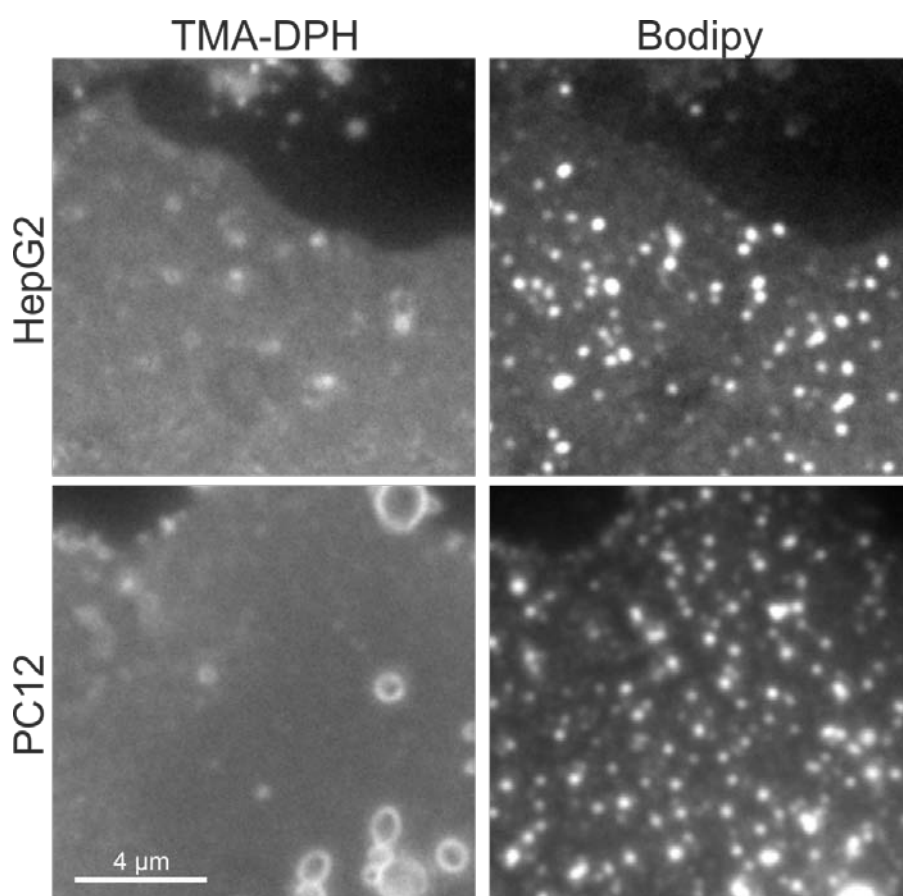

Figure 17. PC forms spots on native plasma membrane sheets.

HepG2 and PC12 cells were fed with propargyl-choline ON and fixed in 4% PFA. After cycloaddition imaging was performed with an epifluorescence microscope visualizing first target membranes (TMA-DPH) and then the signals of pPC (Bodipy) inthe plasma membrane preparations. The left panels show representative membrane sheets visualized with TMA-DPH and the right panels show the same membrane sheets after switching to Bodipy channel.

Similar to the results seen in whole cells, membrane sheets also showed spots after cycloaddition of Bodipy to pPC. Beyond this finding, there is a homogenous layer of labeled pPC indicating that not all pPC is found within spots.

3.3 Does temperature influence the cycloaddition reactionand the formation of pPC spots?

So far, all experiments were performed at RT. Concerning the characteristics of lipids to form phases at different temperatures (Quinn et al., 2005), it was important to carry out a control experiment in which click reaction and imaging were performed at a different temperature. For this reason, physiological temperature (37°C) was chosen in order to confirm, that spot formation is not a result from temperature driven phase formation.

First, membrane sheets were prepared as already described and click reaction was carried out at 37 °C in a humid chamber. Then, aconfocal laser scanning microscope with a moisture and climate control chamber was used for performing imaging. The membrane sheets still show spots (Figure 18). This experiment shows that neither during the click reaction nor during imaging spots are able to form. Therefore a hint is given that spots are not artifacts driven by temperature influence.
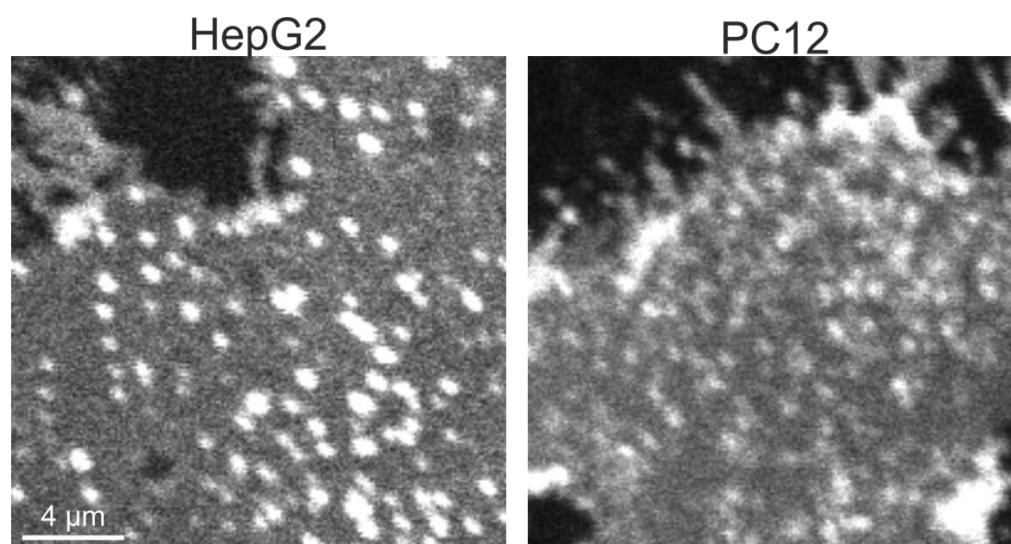
Figure 18.Cycloaddition of azido-sulfo-Bodipy to pPC and imaging at 37 °C.

The left panel shows a representative membrane sheet prepared from a HepG2 cell. The right panel shows a membrane sheet from a PC12 cell. CLSM images show distribution of pPC after click reaction.

3.4Fraction of metabolically labeled pPC by azido-hydroxycoumarin

Mammalian cells synthesize PC via the CDP-choline pathway or the PEMT pathway (see section 1.5.2*Lipid homeostasis*). During this process, propargyl-choline supplemented in the cell media is therefore bioincorporated either into PC or SM. In order to check for the relative amount of pPC related to all lipids with incorporated propargyl-choline.Cells were seeded on 6-well plates, fed and incubated with propargyl-choline for different time periods (0 h, 2 h, 4 h, 6 h, 8 h and 10 h). After the defined incubation time, cells were harvested and lipidswere extracted. The click-reaction was then performed on the samples prior to TLC.

In these experiments, labeling of pPC was performed with azido-hydroxycoumarin (Thiele. et al., 2012). The dye is non-polar and does not dominate the migration behavior of the reaction products during the TLC separation. As a reference lyso-propargyl-PC and propargyl-PC were used. Figure 19shows a representative result after separation of

the clicked samples on a standard silica gel TLC plate. Two distinct solvents with different polarities were used for the separation run (see methods, TLC).

As a standard, no sphingomyelin available for click chemistry so far but characteristic SM double bands run below PC and above lyso-pPC. In case that the propargyl-choline is also incorporated into SM, there should be a stronger fluorescence signal.After 8h, around 98 % of the labeling is seen in pPC, less than 1 % is detected in lyso-pPC as well as in SM (not shown). The ratios did not vary with feeding time. TLC demonstrated that cycloaddition labels almost exclusively pPC even after short feeding times of the cells with propargyl-choline.
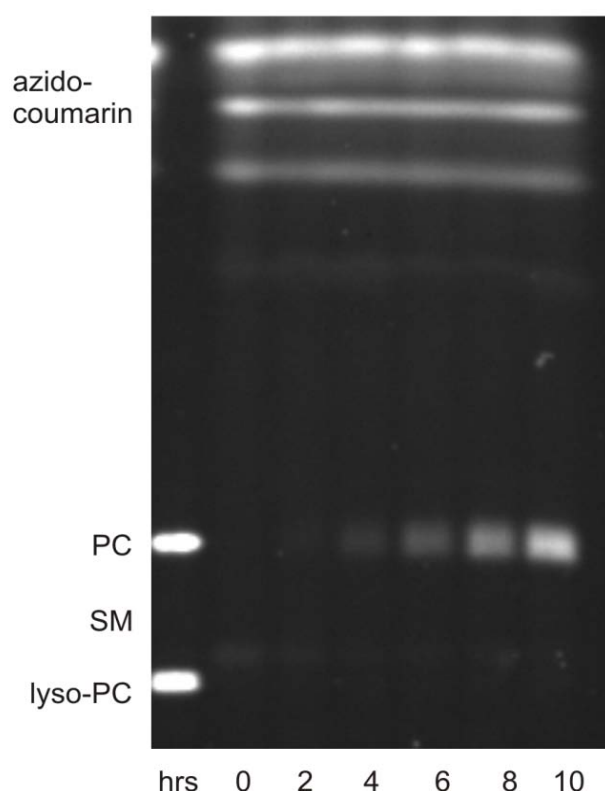

Figure 19. Propargyl-choline is incorporated into propargyl-phosphatidylcholine (pPC).
HepG2 cells were fed with propargyl-choline for 2-10h and lipid extracts were analyzed by TLC. From top to bottom, unspecific azido-coumarin background bands, pPC and lyso-pPC are seen.Analysis of the 8h sampleresulted in 98±0.2%pPC signal andonly very low propargyl-choline signal was detected in SM (0.7±0.1%) and lyso-pPC (0.7±0.2%). Values are given as mean ±SEM (n=5).

3.5Changing pPC concentrations and platforms within plasma membrane of cells

After first characterization of the pPC organization in platforms, the question was addressed whether the domains can be altered experimentally. For instance, number of pPC spots may depend on the level of pPC concentration. To this end, a strategy was designed for changing pPC levels in membrane sheets. It has been already shown that lipid transfer proteins are specific intracellular transporters for lipids (Alpy and Tomasetto, 2005).On this basis,the idea came up to use a specific PC transporter to deplete the lipid from the plasma membrane and then check if after click reaction still spots can be visualized.The lipid transfer protein StarD2 was purified and applied on native membrane sheets priorto click reaction. StarD2 is a cytosolic protein that binds specifically PC taking advantage of its lipid binding pocket that is able to carry one PC molecule that is first removed from a donor membrane (see section *1.5.2 Lipid homeostasis*, Figure 11).

Another idea was to check if spot formation is dependent on proteins. In order to change the number of spots, another strategy was designed from observations made in experiments concerning protein clusters. Ca^{2+} ions have been shown to have electrostatic effects on proteins. As already described (Zilly et al., 2011), calciumincrease led to associations of negatively charged proteinsby compensating local accumulation of electric charges.

In the following two segments the new approaches for experimentally influencing pPC platformsare presented: directly via StarD2treatment for pPC depletion on membrane sheets and byinducing first Ca^{2+} increase in whole cells that are then prepared to membrane sheets.

3.5.1 Do pPC spots form only when a critical pPC concentration is available?

As described in the methods section StarD2 was overexpressed by bacteria and purified in a large scale. Figure 20 shows the western blot analysis. The anti-His antibody(mouse monoclonal IgG (cat. no.: sc-53073, Santa Cruz, USA) was used to detect the protein.The purification was performed using the His-tag attached to the protein. For western blot analysis a sample was taken in all steps of the purification protocol. The protein was always freshly purified for every single assay that it was needed for. Storage at -80 °C in elution buffer supplemented with glycerol led to protein crystallization and is not suitable for this protein.
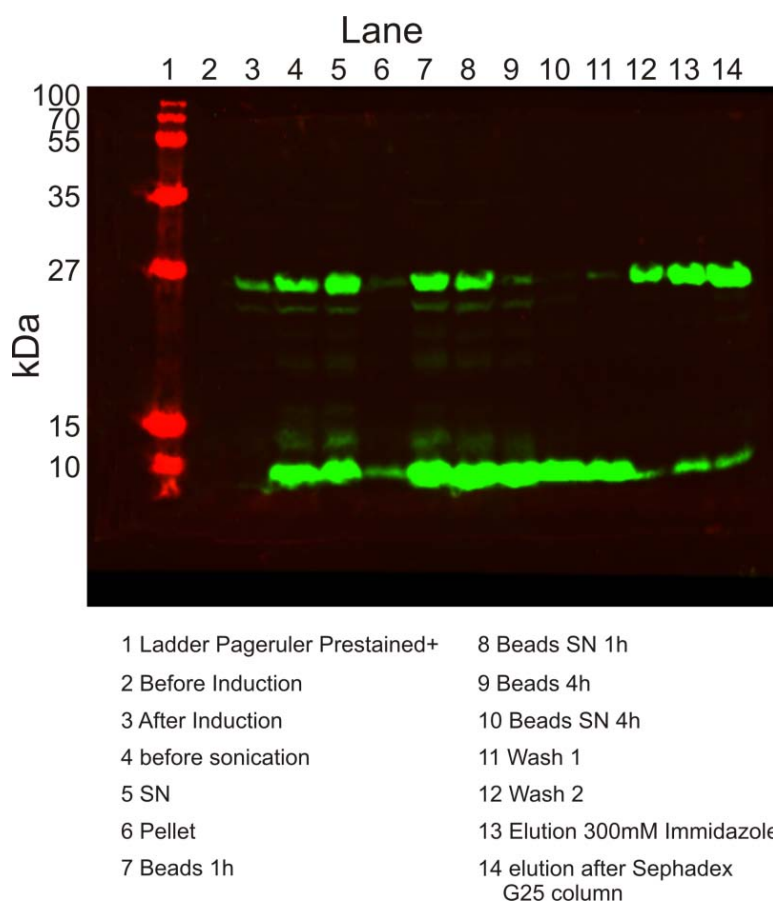

1 Ladder Pageruler Prestained+	8 Beads SN 1h
2 Before Induction	9 Beads 4h
3 After Induction	10 Beads SN 4h
4 before sonication	11 Wash 1
5 SN	12 Wash 2
6 Pellet	13 Elution 300mM Immidazole
7 Beads 1h	14 elution after Sephadex G25 column

Figure 20.Protein purification of StarD2.
In western blot analysis the protein purification of StarD2 can be monitored. Lane 14 resembles the final elution of the 24 kDa sized protein. A clear band slightly below the 27kDa is visible. Lanes 2-13 represent different steps during purification protocol as indicated.

Once the protein was successfully purified, the protein was freshly applied on HepG2 membrane sheets. Astonishingly, pPC was almost decreased by half when applying merely 100 nM of StarD2. Figure 21A shows representative images of membrane sheets prior and after incubation with StarD2. The treatment of StarD2 decreased the overall intensity of the signal, but the spots were still present after using 100 nM and 250 nM StarD2. The use of higher concentration had already effects on the integrity of the membrane sheets. This disintegration was observed by TMA-DPH staining (data not shown) in form of holes within the membrane sheets.
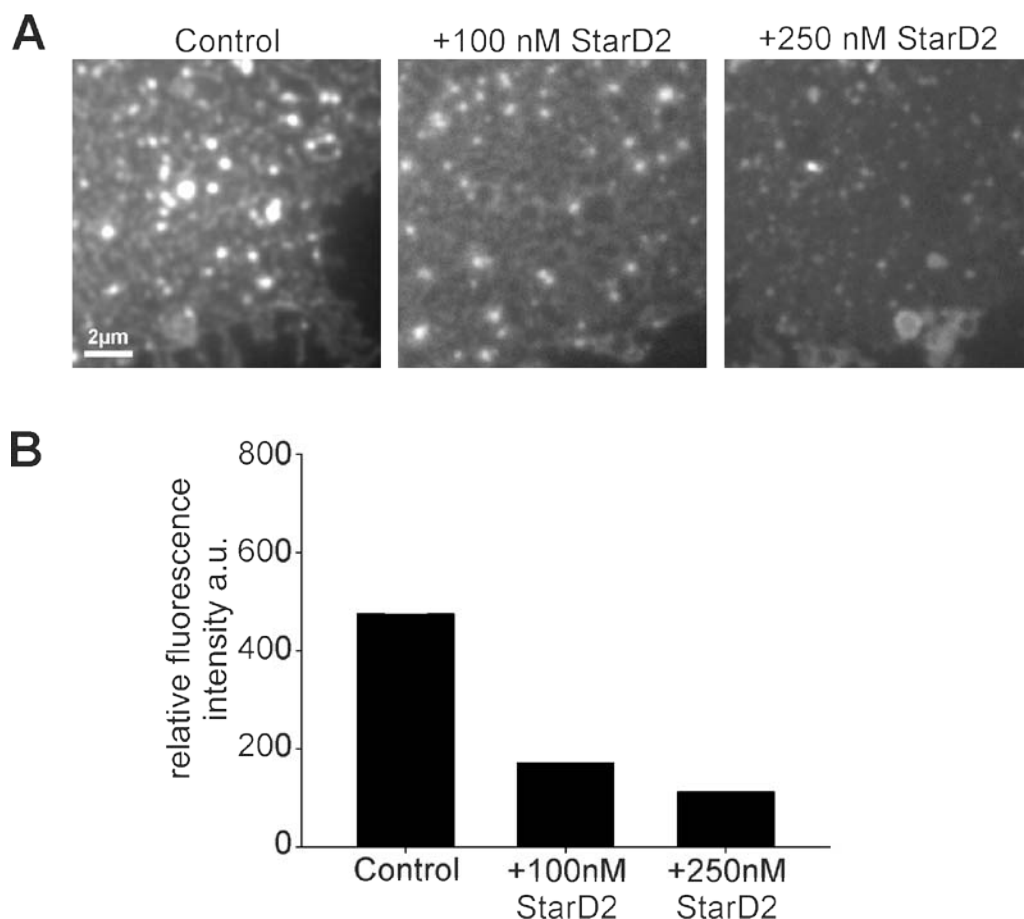

Figure 21. Depletion of pPC from membranes by StarD2.
Representative membrane sheets from HepG2 cells in control condition without StarD2 treatment (A) and membrane sheets after 5min incubation with 100 nM or 250 nM StarD2 at 37 °C. A loss in fluorescence is detected (B) compared to control conditions (475 ±232 a.u.) to 100nM StarD2 treated membrane sheets (171 ± 141 a.u.) and 250nM (112 ± 47 a.u.) treated membrane sheets; experiment with 21-29 membrane sheets measured per condition).

This preliminary data suggests that even though half of the pPC is removed spots persist.

3.5.2 Intracellular increase of calcium decreases PC spots and overall intensity

As already mentioned, it should be tested if the intracellular increase of calcium concentration also has an effect on the organization of pPC. Therefore, HepG2 cells were seeded and fed ON with propargyl-choline. Then, cells were treated with the ionophore ionomycin in order to transport and therefore increase Ca^{2+} ion concentrations (see Methods, section*2.2.11*). Membrane sheets were then prepared and click reaction was performed for labeling of pPC. The images of representative membrane sheets are shown in figure 22.
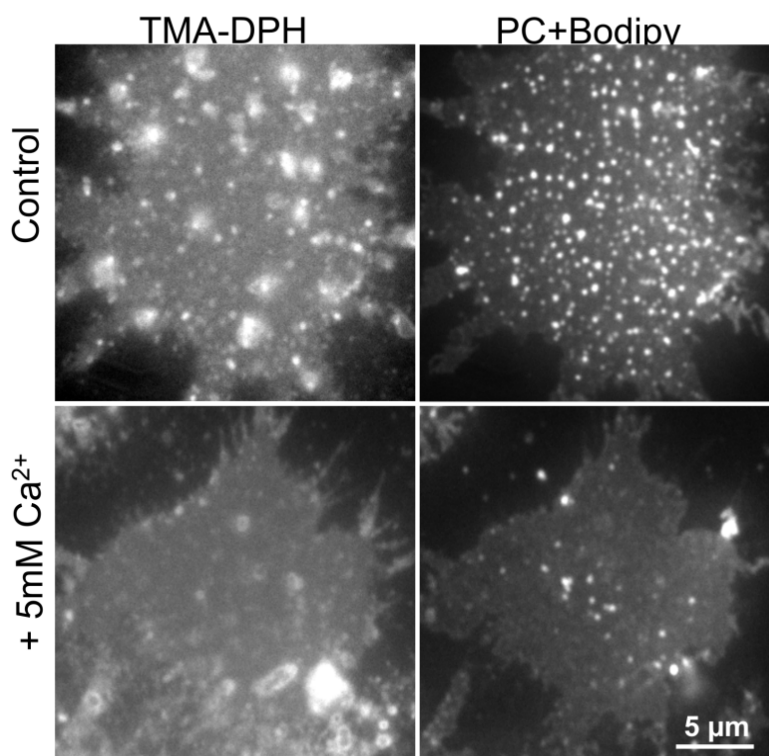

Figure 22. Influence of calcium ions on pPC organization.
Intracellular levels of calcium ions were increasedin HepG2 cells by treatment with ionomycin and membrane sheets were prepared. TMA-DPH was used for visualization of membrane sheet integrity (left panels) and Bodipy coupled to PC was detected after click reaction (right panels). The effect was not quantified but seen in the experiments. (n=3 experiments, each with 15 membrane sheets imaged) Figure shows representative membrane sheets.

The membrane sheets of the control show the typical abundant pPC spots and the homogenous layer. When Ca^{2+} was intracellularly increased, the sheets prepared from those cells showed a significant decrease in spot number and a lower intensity in fluorescence was measured (Figure 23). This experiment shows that pPC spots are probably kind of dependent on protein organization. In addition, the experiment shows that spots are dependent on biological mechanisms and not a result from the cycloaddition reaction as in both conditions membrane spots are identically treated after sonication.
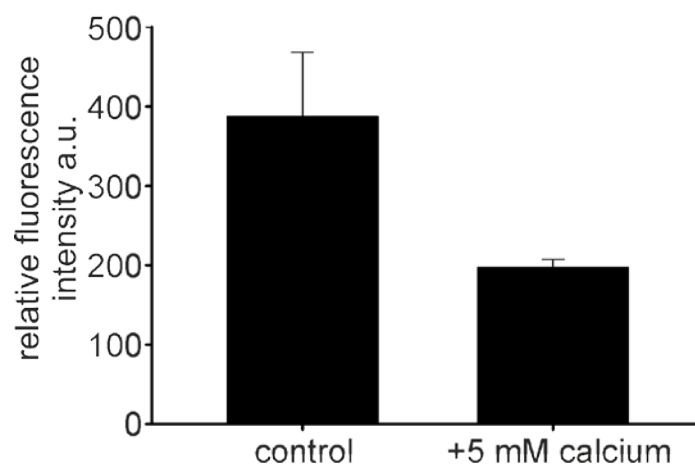

Figure 23.Quantification of loss in fluorescence signals of labeled pPC induced by calcium. Graph shows the relative fluorescent intensity of labeled pPC in control or increased calcium conditions. The relative fluorescence signal obtained from the control condition was 548 ±81 a.u. and the signal decreased to 255 ±10 a.u. after Ca^{2+} increase. (n=2, 5-24 sheets were measured on each experiment, values are given as mean ±STD)

As already mentioned above, calcium ions were shown to be able to influence the arrangement of membrane proteins.In the case that proteins recruit pPC into platforms, a disturbance of the protein order would also influence pPC organization. This possible interaction between proteins and pPC might explain the reduction of spots found within the PM after calcium treatment.

The calcium effect was described for some SNARE proteins (Zilly et al., 2011). Interestingly some of these proteins are also known to be dependent on cholesterol rich phases within the PM (Lang et al., 2001).

Propargyl-PC could be another lipid that co-stabilizes SNARE complexes.In order to check if pPC spots are also associated to SNARE proteins a colocalization coefficient was calculated. The Pearson correlation coefficient (*cc*) was calculated as described in the methods section. The coefficient defines the degree of a linear correlation between fluorescence signals distributed in two images (Manders et al., 1992). In case of 100 % colocalization a Pearson correlation coefficient would be *cc* = 1. This is the case in two identical images. The inversion would result in a correlation coefficient of *cc* = -1. If two images do not correlate the *cc* value is 0. For colocalization experiments, membrane sheets from HepG2 cells were prepared as already described and after click reaction an antibody staining was performed.
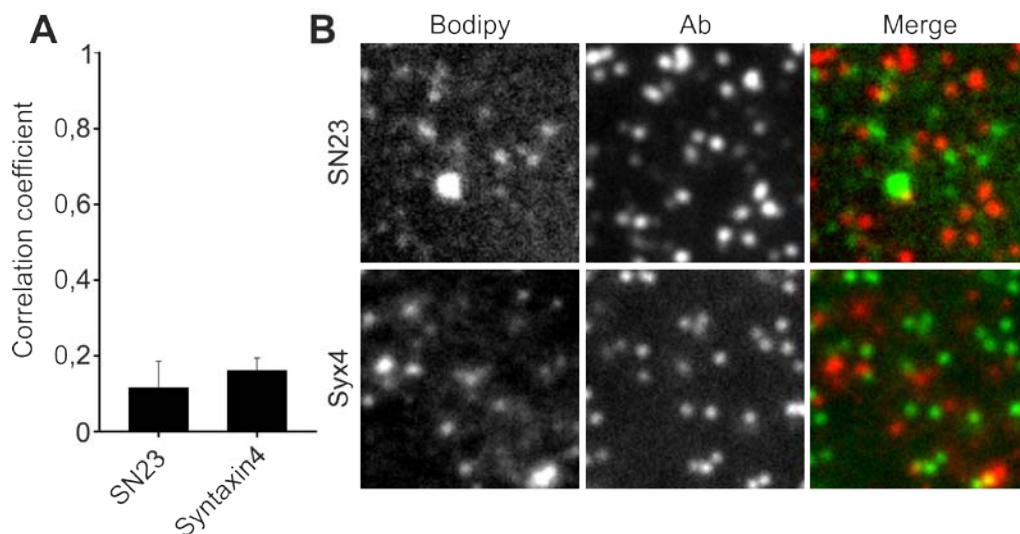

Figure 24.Colocalization analysis of pPC with SN23 and Syx4.
(A)Graphshows the Pearson correlation coefficient from the colocalization experiments. SN23 0.1 ± 0.03; Syx4 0.16 ± 0,03 (n = 3 experiments, 66 - 101 membrane sheets were measured. Values are given as mean ±SEM). (B) Membrane sheets of HepG2 cells were prepared as already described. Prior to cycloaddition, immunolabeling was performed using antibodies against different proteins of interest (SN23, Syx4). The membrane sheets were then imaged in the different channels (TMA-DPH –not shown, Bodipy, Cy5). The left panels show the structures from the pPC of representative membrane sheets. Central panels show the Ab labeling signal of the corresponding protein. The right panels show a merged image of both channels, demonstrating only little colocalization of the pPC vs. the tested proteins.

The colocalization analysis of pPC spots vs.SN23 and Syx4 showed no correlation between the staining of pPC and the respective protein. This result means that the tested SNARE proteins are not connected to pPC spots.

3.6Imaging of PC spots with super-resolution microscopy

The labeling of pPC on cells and membrane sheets showed a novel organization level of the lipid on the plasma membrane of cells. In order to characterize the spots in more detail super-resolution microscopy was applied. STED microscopy was used for exact visualization of morphology and size of pPC spots. HepG2 cells were prepared as already described and again a click reaction was performed, but for STED microscopy it was necessary to utilize a different fluorophore. In this case, an azido-coupled Atto647N dye was applied for click-chemistry.For illustration of the gain in resolution, first a CLSM image was taken (Figure 25) and then the setup was switched to STED mode in order to improve resolution and quality of images. Signals of spots that might appear as one big spot observed by CLSM on a membrane sheet preparation can now be distinguished by STED as two or more spots.
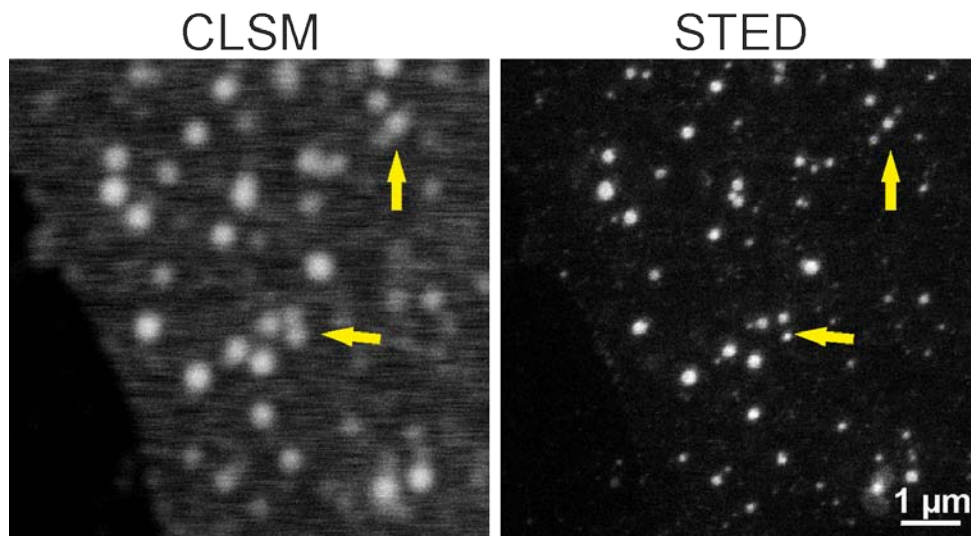
Figure 25.Imaging of labeled pPC with CLSM vs. STEDmicroscopy.

The spatial resolution of microscopy images is strongly improved by STED microscopy compared to conventional CLSM. The yellow arrowsmark regions where pPC structures areobservedin CLSM (left panel). The same region was then acquired after switching to STED mode (right panel). The yellow arrows demonstrate that the marked spots in CLSM in fact consist of twowhen viewed in STED mode. These experiments were performed at the European Neuroscience Institute in collaboration with the Laboratory of S.O.Rizzoli. S. Saka performed the imaging of two experimental days of data shown in figure 26.

However, in general STED microscopy was not necessary to resolve spots but more important required to visualize the exact size of the spots and therefore improve accuracy of the analysis. Figure 26shows the analysis of the spot size. Once a ROI is defined, a linescan (3x30 pixels) is laid centered over single spots (Figure 26B). The length is also important for having a base line on the fluorescence intensity profile acquired for each spot so thata gaussian fitting can be performed afterwards (Figure 26C). Gaussian half-width corresponds to real spot size (Bill et al., 2010). The analysis of spot sizes resulted in an average size of 122nm$\pm$16nm.
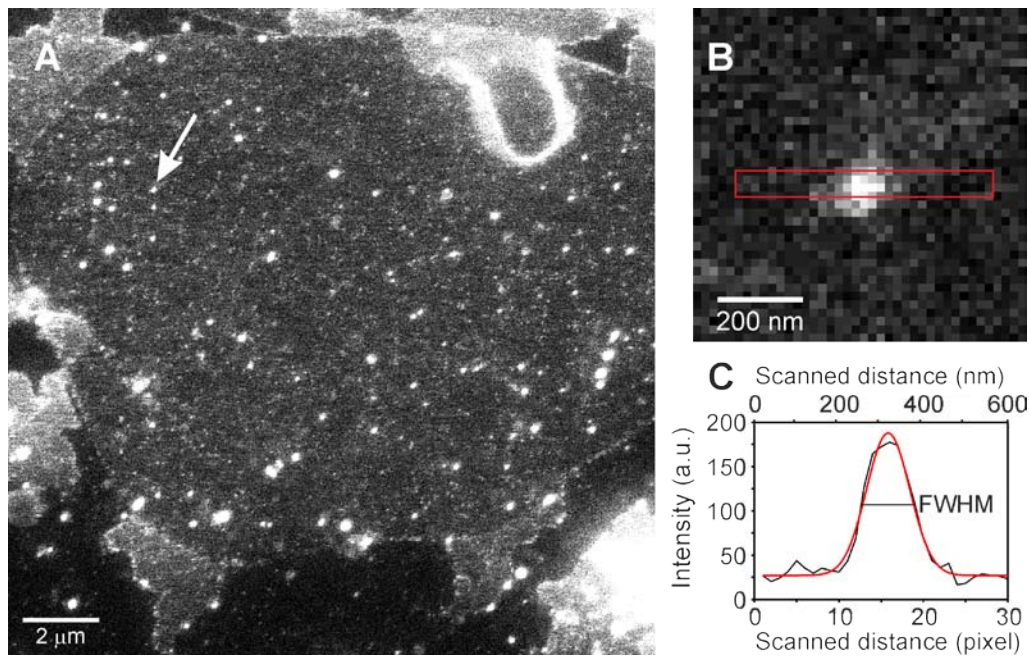
Figure 26.STED microscopy of ATTO647N-labeled pPC and analysis of single spots.
A representative STED image of pPC in a native plasma membrane preparation of a HepG2 cell.From individual spots (B, shows spot indicated by arrow at different constrast), linescan analysis was performed. Intensity profile was fitted to a Gaussian distribution from which the full width at half maximum (FWHM) was obtained, resulting in 122 ±16nm which corresponds to the size of the spot (n=3 independent experiments; for each experiment 122-259 spots from 17-25 membrane sheets were analyzed). Value is given as mean ±SEM.

From the imaging experiments using STED microscopyit is possible to use the same data for calculation of the enrichment factor of the pPC spots in contrast to the homogenous layer of labeled pPC within the plasma membrane (Figure 27).An averaged enrichment of 236 ±68% could be calculated for pPC spots. It should be noted that the enrichment calculation could be an underestimate due to quenching of the Bodipy fluorophore preferentially occurring in the densely crowded spots, so the real value is in fact much higher.
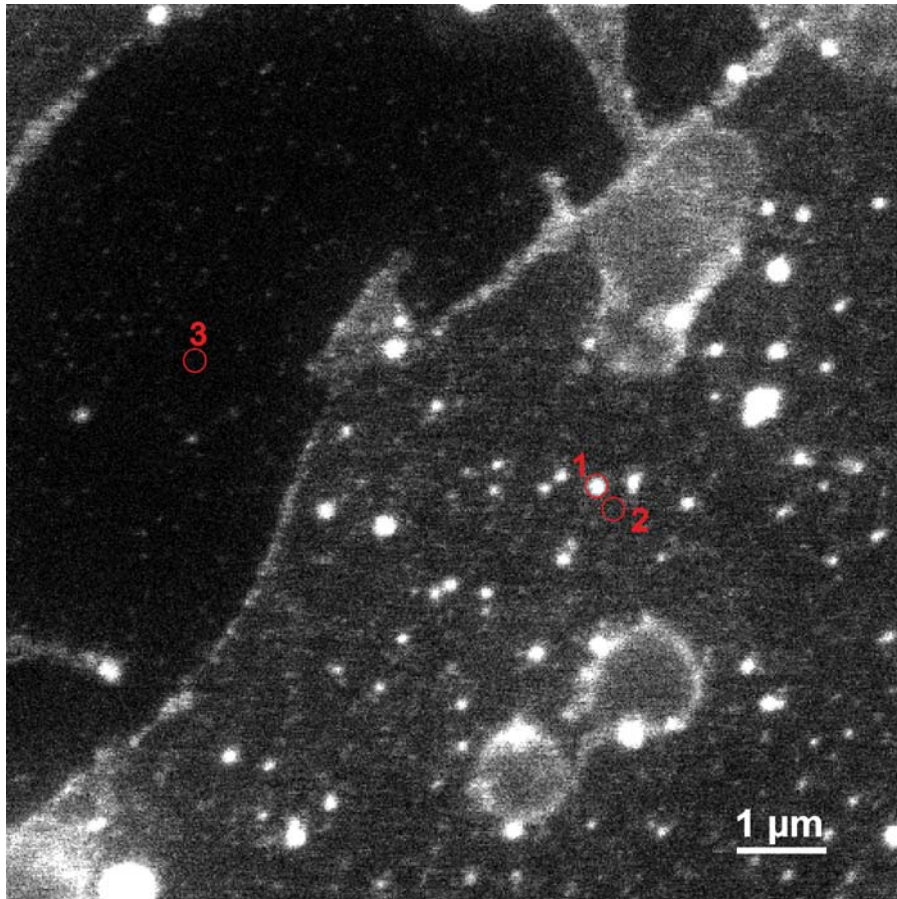
Figure 27.Enrichment of pPC quantified bySTED microscopy.

For quantifying the enrichment of pPC spots in comparison to the homogenous membrane, the same spots wereselected as in spot size analysis. A representative STED micrograph is shown on which the sites of the three measurement ROIs are marked: a PC spot in the membrane (1), the homogenous layer the closest possible to the spot (2) and the background that is used for correction of the values (3). Calculations resulted in an average enrichment of 236 ± 68 % (n = 3; for each experiment 182 - 314 spots from 17 - 25 membrane sheets were analyzed). The value is given as mean ± SEM.

In summary, the results achieved by high resolution microscopy show again a spot formation by pPC on the plasma membrane of cells. The spots are very numerous and dispersed all over the membrane samples but do not move.No specific pattern or order of the spots could be identified. The spots were calculated to be 120nm in size and the enrichment factor of pPC spots showed a 236% higher concentration of pPC in comparison to the surrounding homogenous layer.

3.7 pPC is mobile within the plasma membrane of cells

Lipids and proteins are mobile within the PM of cells. Analysis of dynamics is important in order to check whether the molecules within the pPC spots exchange lipids with the surroundings. The displacement might be hindered by surrounding within the membrane or by cytoskeletal structures associated to the PM. FRAP is a commonly used microscopy method for the analysis ofdiffusional mobility of membrane components. Usually, fluorescent proteins (e.g. EGFP) are used in FRAP but in principle all fluorophores that can be bleached are suitable for this method. The azido-sulfo-Bodipy used for click chemistry hassimilar excitation and emission curves as GFP and can thereby be bleached in the same manner.

For testing the dynamics of pPC, cells were seeded on glass coverslips and fed over night with propargyl-choline. The next day, membrane sheets were prepared and the click reaction was performed. After cycloaddition of the azido-sulfo-Bodipy the sample was analyzed on a CLSM with a FRAP module that permits the bleaching of a defined ROI within the field of view.In the case of the clicked pPC it could beconfirmed that lipids move fast on the PM.An interesting observationwas made in one of the first FRAP experiments in which not only fast recovery of the homogenous layer containing pPC was observed but also in the enriched spots. Figure 28shows the recovery of such a spot within seconds.
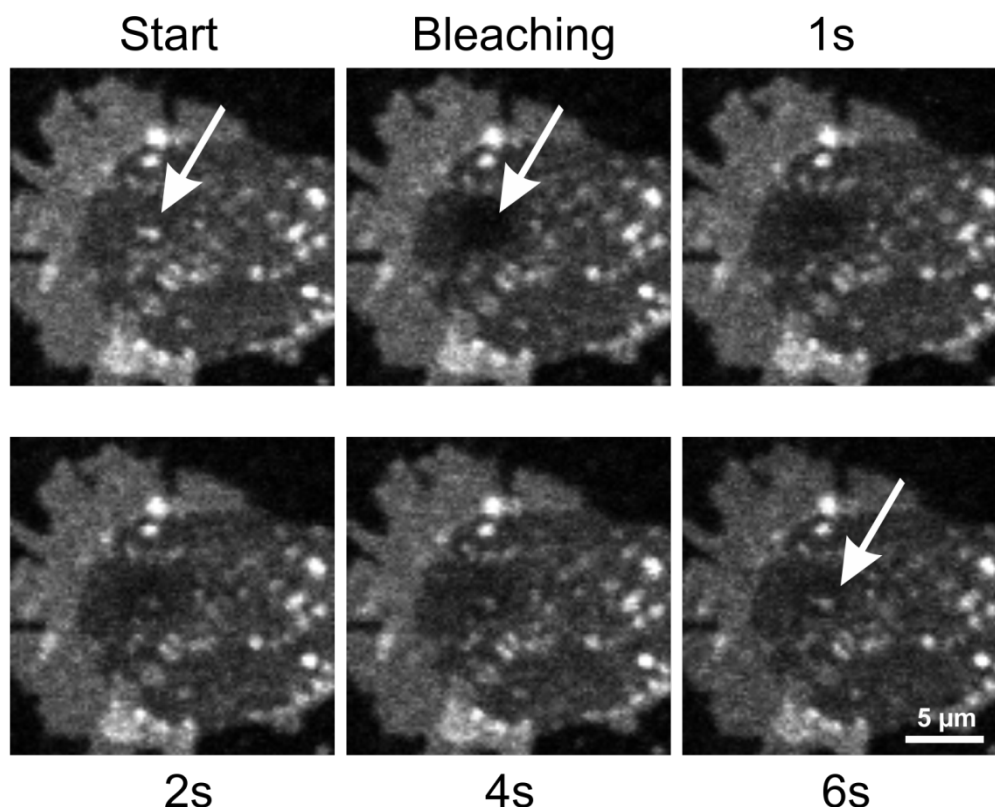
Figure 28. FRAP of pPC on membrane sheets of HepG2 cells.

Native membrane sheet acquired with a confocal microscope. PC fluorescence in a defined squared ROI (30x30 pixels)was bleached and five more images were acquired.The arrow marks the region of interest bleached in this FRAP experiment.

The fast diffusion of lipids within membranes has been already shown in earlier studies, so this question was not addressed when establishing a new FRAP protocol. In the first observations, the spots remained static and were able to recover. A new reduced FRAP protocol was then established as described in the methods. The protocol includes shorter acquisition times because of the bleaching effects of the Bodipy labeling to the pPC. The new question that arose was whether there is exchange between platform molecules and their surroundings. The new designed experiments should answer this. It cannot be excluded that Bodipy has an influence on the overall diffusion dynamics.

In order to control for spontaneous recovery of the Bodipy dye, the FRAP protocol was applied on whole membrane sheets (Figure 29). Under the established experimental conditions, at least two membrane sheets were imaged with the exception that not a ROI was bleached but

one entire membrane sheet. Under these conditions no recovery was observed, documenting that the recovery seen in figures 28, 30 and 32 are the result from unbleached molecules diffusing into the bleached area.
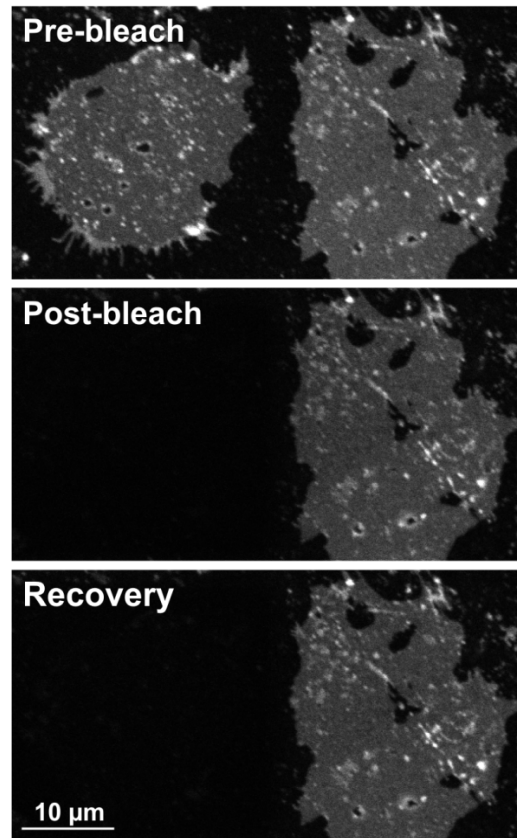

Figure 29. FRAP control for labeling of pPC on membrane sheets. The figure shows a representative pair of plasma membrane preparations.Membrane sheets of HepG2 cells were prepared as already described and after cycloaddition of Bodipy to pPC the samples were used directly for FRAP experiments. For this experiment, a bigger ROI was set for visualizing two whole membrane sheets (pre-bleach). Then a bleaching ROI was placed over a whole membrane sheet and an image was acquired after bleaching(post-bleached). After 60 s a final image was acquired (recovery). (n = 3, each experiment includes 5 membrane sheets)

It was thencalculatedhow manybleached PC spots are able to recover with unbleached labeled PCin the ROI. The FRAP protocol generates a pre-bleach image where a ROI for bleaching is randomly set on the homogenous layer of the plasma membrane preparation. Bleaching then was followed by immediate image acquisition (post-bleach). 60s after initiation of bleaching another image is acquired for visualization of the fluorescence recovery (recovery). Figure 30 shows the results from application of the new FRAP protocol on native membrane sheets.

Ahistogram demonstrating the distribution of the amount of fluorescence recovery on the level of individual nanostructures is shown in figure 30. The levels of recovery differ: some spots recover slightly while others recover almost to the initial intensity. All in all, most spots recovered significantly and remained static. Spot enrichment was calculated as already described for STED imaging and recovery intensity was related to pre-bleach intensity yielding %-recovery. The results are shown in figure 30 (lower panel).
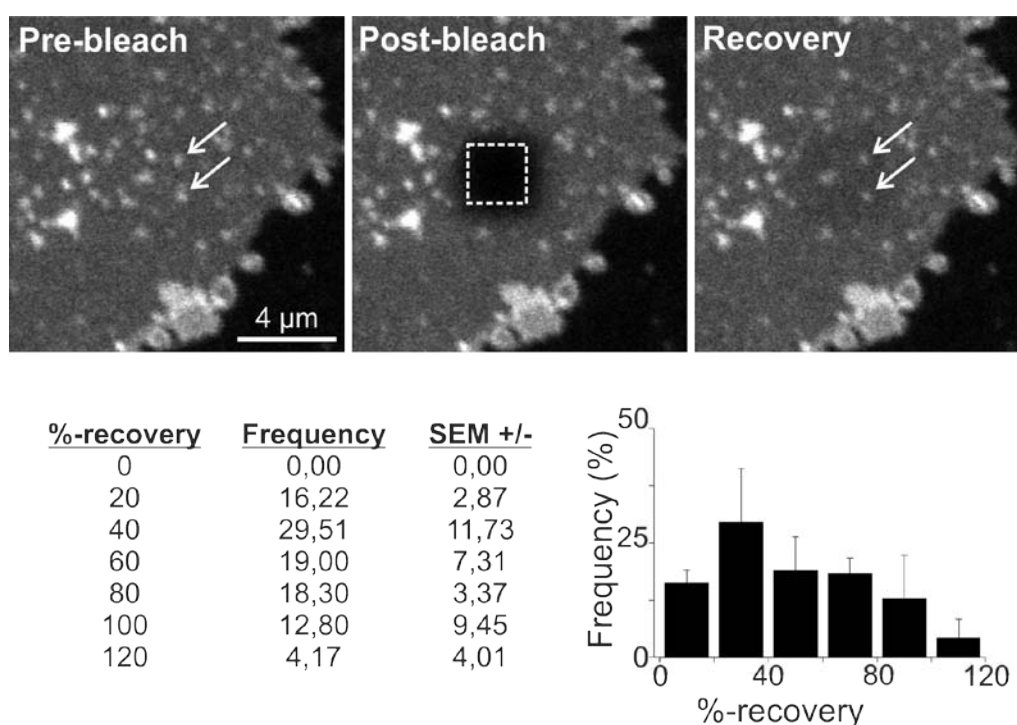

%-recovery	Frequency	SEM +/-
0	0,00	0,00
20	16,22	2,87
40	29,51	11,73
60	19,00	7,31
80	18,30	3,37
100	12,80	9,45
120	4,17	4,01

Figure 30. FRAP analysis of pPC on native plasma membranes of HepG2 cells. Upper panelsshow arepresentative membrane sheet and the different acquired timepoints of the images.In the pre-bleach and the recovery image, fluorescence arising from spots was corrected for uniform background fluorescence. The calculation for the recovery of the spots was performed as described in the methods section. For individual spots fluorescence intensity after recovery was expressed as percentage from the pre-bleach value. Histogram (lower right panel, results are seen in the table to the left) shows the distribution of the extent of fluorescence recovery on the level of individual platforms (n=3, each experiment includes 14-28 spots measured on 5-13 membrane sheets). Values are given as mean ±SEM.

Combining the results obtained so far (%-recovery of spots and the calculation of the enrichment factor as in STED) no correlation could be established between the percentage recovery and the enrichment of

PC. The results are shown in figure 31. For correlation analysis all spot values that show at least 50 % higher intensity than the surrounding were included.
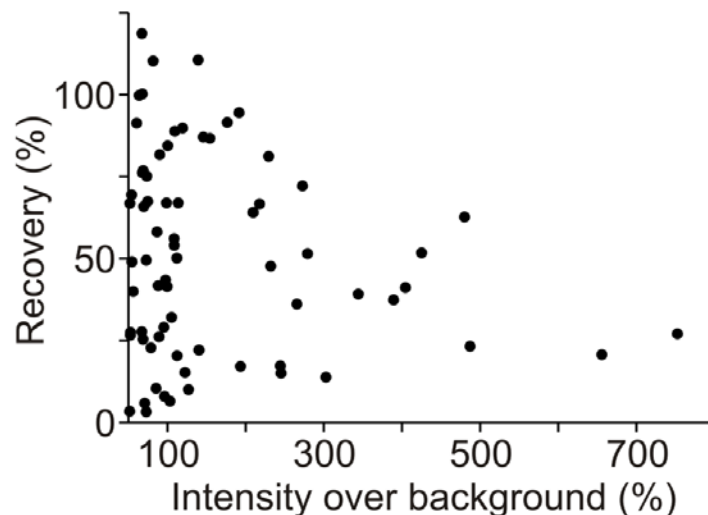

Figure 31.Correlation of pPC enrichment factor vs. recovery.
Intensity of single PC spots over homogenous background (x-axis) was plotted versus the recovery percentage (y-axis). In this graph all spots from 3 independent experiments were included that show a minimum of 50% intensity over the background (n=3experiments, 72 spots >50% enrichment factor).

The FRAP experiment shows that PC spots exchange molecules with their surroundings. In addition, it can be concluded that the spots are not organelles associated to the PM because those should not recover after complete bleaching.

3.8Does fixation influence the recovery of lipid spots?

The results so far show that on native plasma membrane sheet preparations PC molecules diffuse.The observed spots with enriched fluorescent signals from pPC recovered after FRAP analysis. An interesting question to solve was if the commonly used fixative PFA would influence this recovery. PFA is a fixative agent that denaturates proteins and thereby terminatesbiochemical reactions. Fixation of cells has been shown to have no effect on the dynamics of lipids (Kusumi and Suzuki, 2005). For testing this, HepG2 membrane sheets were prepared and fixed prior to the click reaction or after performing

cycloaddition. As shown in figure 32, in both cases fixation reduced recovery modestly. The recovery images did not show a high amount of recovery as seen in the native plasma membranes, an imprint remains in the ROI that was bleached.
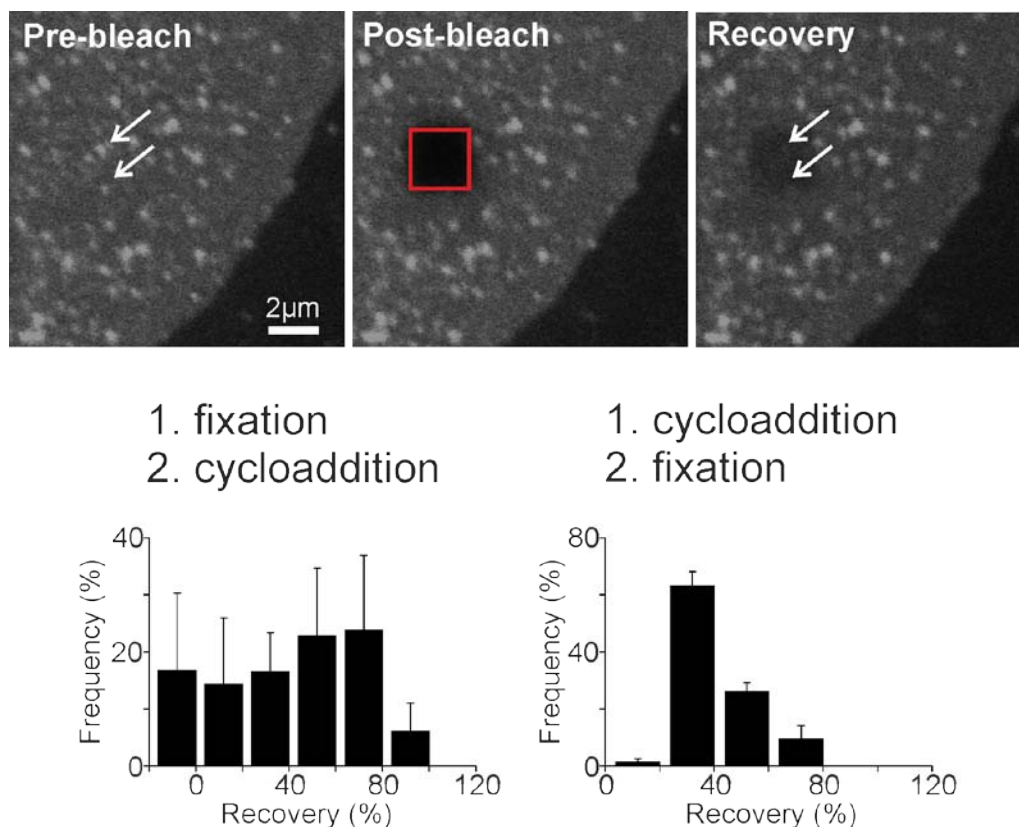

Figure 32. FRAP analysis of membrane sheets including PFA fixation before or after labeling of pPC. Membrane sheets of HepG2 cells were prepared and fixation occurred before or after the click reaction. The upper panel is representative for images obtained after applying the FRAP protocol on membrane sheets that were fixed after click reaction. The arrows mark spots that recover after bleaching. Lower panels show the histograms of the different conditions of fixation before (left histogram, n=3, each experiment includes 6-14 spots measured on 3-4 membrane sheets) and after (right histogram, n=3, each experiment includes 5-24 spots measured on 4-9 membrane sheets) click reaction. Values are given as mean ±SEM and only spots with enrichment factor >50% were included.

Enrichment factor and recovery rate were analyzed for correlation as describedfor native membrane sheets.Again, no correlation could be observed (Figure 33).
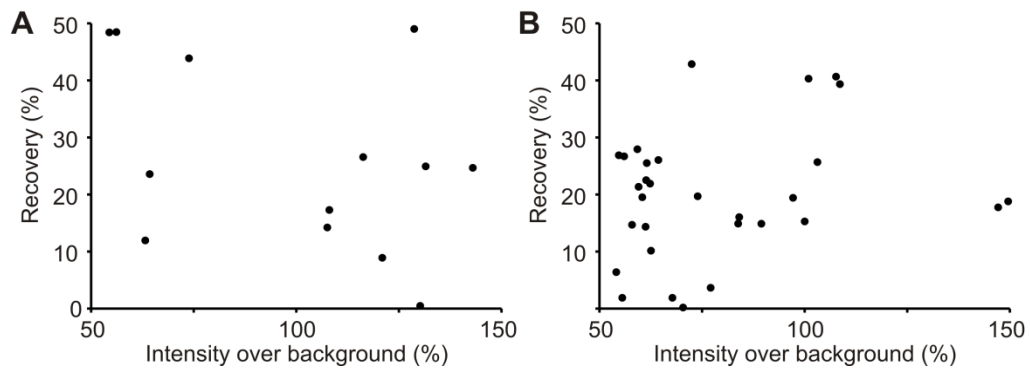
Figure 33. Correlation of pPC enrichment factorvs. recovery on fixed cells. Graphs show the correlation of recovery vs. enrichment factor of pPC spots fixed before (A) and after (B) the click reaction. Intensity of single PC spots over homogenous background (x-axis) is plotted versus the recovery percentage (y-axis). In this graph all spots that show a minimum of 50% (and up to 150%) intensity over the background are included. These are the major populations encountered in the analysis. Therefore the number of spots presented in the range is reduced in comparison to the native plasma membrane preparations (for A, n=3 experiments, 13 spots >50% enrichment factor; for B, n=3 experiments, 30 spots >50% enrichment factor).

In summary, pPC was demonstrated to diffuse across the PM in fixed preparations.The pPC found within the spots exchanged with its surrounding but the spots themselves remained stable and static. There was no correlation of the enrichment factors to the recovery percentages and fixation only had a moderate effect on the diffusion of PC molecules in the PM. The data obtained from FRAP suggests also that there is no enzymatic activity required for pPC spot formation.

3.8.1 Lipid platforms diffuse on the PM of membrane sheets after incubation with trypsin

In order to show the dependency of the lipid platforms on proteins and check if the spots can be destabilized in any manner, membrane sheets were incubated with trypsinafter click reaction. The unspecific cleavage of proteins by this enzyme resulted in liberation of the spots that started floating on the PM after less than a minute. The spots have distinct mobilities and those spots that were close to the membrane border

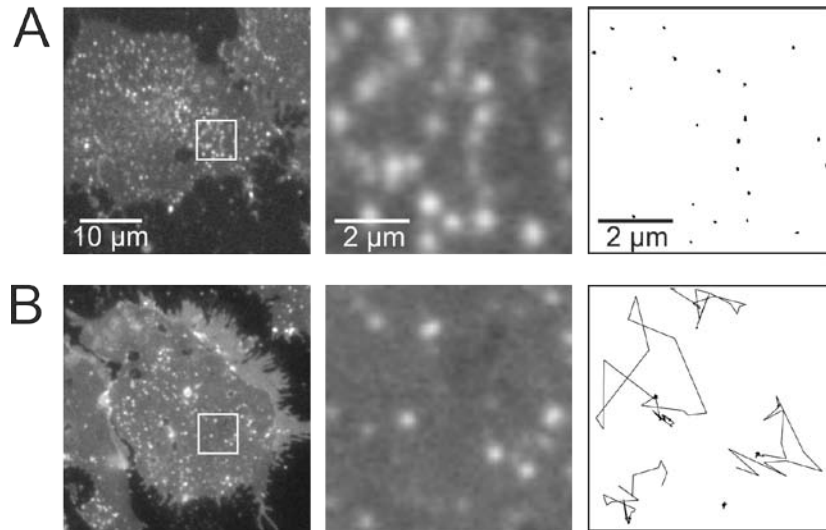didnot disappear, but moved along the edge or back inwards again (personal communication Elisa Merklinger).

Figure 34. Trypsin treatment of membrane sheets after click reaction. Epifluorescence microscopy of native membrane sheets after addition of trypsin. Left column shows representative membrane sheets with labeled pPC platforms, in the middle a magnified view includingthe platforms that are tracked by the analysis. Right column illustratesthe tracks from the platforms over a treatment period of 200s. Diffusion coefficients were calculated from linear regression lines resulting in values of 0.311 x10^{-4} µm^2/s (control) and 8.56 x10^{-4} µm^2/s (trypsin).Result was obtained in collaboration with E. Merklinger and J.G. Schloetel. E. Merklinger performed the experiment and J.G. Schloetel the analysis. Figure was provided by E.Merklinger, J.G.Schloetel and T.Lang. (Spitta et al., 2012)

In summary, the data suggest that protein networks immobilize the PC structures on the plasma membrane of cells. In a long-term treatment of the membrane sheets with trypsin (incubation at RT for 45 min) the spot number diminished but this effect is probably the effect from longer incubation with the enzyme (personal communication of Elisa Merklinger). The proteolytic reaction is very efficient and therefore the networks destabilize that maybe recruit the pPC.

4.   Discussion

In this work, a new level of organization of the phospholipid PC is presented resulting from studying pPC. Propargyl-PC forms stable long-lived lipid platforms and these platforms were visualized on whole cells and on native plasma membrane preparations. The platforms were characterized in size (120 nm) and an enrichment factor was calculated (236%). The dynamics of the platforms were addressed by demonstrating that they exchange the pPC molecules with their surroundings.Formation does not depend on the pPC level and most likely involves proteins. Though dynamic, they do not move laterally in the plasma membrane. Moreover, the results obtained by collaborations demonstrate that the lipid platforms can be destabilized by long term enzymatic treatment with trypsin. This result gives another hint that there must be a protein lipid interaction mechanism that is not fully understood.

4.1 Click-chemistry – is it suitable for visualizing PC platforms?

Click chemistry is a reliable, quick and easy method for labeling the non-genetically encoded lipids.In fact all the advantages that were first predicted when the term click-chemistry was introduced already a decade ago (Kolb et al., 2001), are supported by the experiments in this work and it is because of versatility reasons (click chemistry is not only used in biological research) that this method is gaining rapidly popularity in many research areas (Tian et al., 2012; Yang et al., 2012; Faugeras et al., 2012).As observed in this work, after cycloaddition of azido-Bodipy and azido-ATTO647N to pPC, the labeled lipid could be detected in all microscopy setups utilized for analysis. The effectiveness of the reaction was demonstrated simply by the fact, that fluorescence could be detected within whole cells and distributed in cellular structures e.g. the endoplasmic reticulum. The use of membrane sheet

preparations helped to visualize pPC on the basal PM of cells. This means that after bioincorporation of propargyl-choline into pPC cells still transfer pPC to the PM. So far, lipid labeling has been commonly achieved by chemically introducing a fluorophore (e.g. NBD) to the fatty acyl chain, sometimes even substituting almost the whole acyl chain of a lipid. These lipids are then utilized in experimental approaches (e.g. McIntosh et al., 2010). The biochemical properties of such lipids are strongly influenced by the corresponding fluorophore. Not only steric hindering or reordering might occur when such lipids are incorporated into the membrane. This is not the case with the method presented in this work. The biochemical properties of pPC synthetized from uptake of propargyl-choline should remain equal since the small alkyne group on the choline is only required when cycloaddition of azido-sulfo-Bodipy or another azido-coupled fluorophore to pPC is performed. This makes the presented click-chemistry approach a less invasive method, since the lipid is first metabolically labeled and then for experiments the fluorophore is introduced when required. Nevertheless, on the one hand it cannot be excluded that Bodipy interferes on the surrounding above the headgroup of the lipid, but on the other hand this is rather unlikely because ATTO647N that carries a different charge shows similar spots.

Phosphatidylcholine is the most abundant phospholipid within mammalian membranes (van Meer and de Kroon, 2011). The labeling efficiency on the thin layer chromatography analysis supports the view that spots represent pPC and not another labeled lipid (analysis showed 98% labeling of pPC to only 1 % SM and lysoPC). Interestingly, the same ratio of labeling was detected for all time points of incubation (2h, 4h, 6h, 8h and 10h). Data was not shown on which cells seeded on coverslips and fed with propargyl-choline were sonicated and then click reaction was applied in order to image these samples with different incubation times (2h – 10h) Already in the 2h feeding time, cells managed to bioincorporate the propargyl-choline into pPC and spots could be visualized. This suggests a rapid metabolism of the choline.

Click-chemistry is a suitable tool for visualizing pPC nanodomains. This successful visualization of labeled pPC after click reaction with modern microscopy techniques enabled a detailed study concerning the lateral organization of pPC within the PM.

4.2 PC organization in an authentic lipid raft

After cycloaddition of azido-sulfo-Bodipy to pPC spottiness was detected in whole cells and on membrane sheet preparations. In the images from the original publication (Jao et al., 2009) spots within cells representing presumably cellular organelles could be seen, but it was not expected to find spotty signals within the PM.

The first addressed question was whether platforms are majorly composed of pPC. Enrichment calculations showed a 200 % increase over the uniform layer. In order to test whether pPC platforms exclude other types of molecules because of dense packing different membrane dyes were utilized for colocalization analysis (RedCell Mask, R18 and TMA-DPH). Based on their physicochemical properties, the distinct membrane dyes should also localize within the platforms to similar extent. But this was not the case. They showed low or little einrichment within the pPC spots (personal communication of E. Merklinger and T. Lang). The result is in line with the idea that PC is the key component of the observed platforms.

However, the enrichment could also be a result of docked organelles rich in pPC or vertical accumulation of pPC in membrane invaginations. But colocalization with markers for membrane invaginations such as Clathrin and Caveolin-1 was low (personal communication of E.M and T.L).Spots are also not docked organelles because in FRAP analysis, if enrichment was also due to an organelle or a binding vesicle, then no recovery should be detected, because unbleached pPC molecules cannot reach the organelle. The pPC platforms are no artifacts that might be created by a pPC phase because when performing the click

reaction and imaging at 37°C the spots were still present. The trypsin experiment supports the concept that pPC spots are true lipid rafts that are able to float as a unit on the plasma membrane.

The results support the hypothesis that pPC spots are authentic platforms and not membrane invaginations or docked organelles.

4.3 PC and cholesterol, two players from the same team with different characteristics

Cholesterol and sphingomyelin have been vastly studied due to their assumed participation in the formation of membrane rafts. Simons and Ikonen describedthese two lipids to be the major driving forces for formation of the rafts, but so far there is no exact characterization for example packing density and the amount of cholesterol/SM that are present in the nanometric raft assemblies.Depletion of cholesterol from membrane sheet preparations on which pPC was labeled showed a decrease of pPC spots (personal communication of I. Lauria, Spitta et al., 2012). This result suggests that pPC might be also located or related to cholesterol-rich phases. Nevertheless, a true dependency of PC to cholesterol or vice versa could be analyzed by specific manipulation of the lipid concentrations within membranes. Therefore, the use of lipid transfer proteins will confirm a dependency. Proteins like StarD1 or StarD2 that are capable of binding to just one specific lipid (cholesterol and PC respectively) will help to precisely manipulate the membrane composition.

Cholesterol was described as a lipid that stabilizes the plasma membrane and influences its rigidity while PC has been only described as a rather neutral membrane component. So far, the only relation that has been shown for these two lipids is that cholesterol packs PC at higher densities in bilayers (Xu and London, 2000; Hub, et al., 2010).

4.4 Mechanism of PC platform formation and its biological role

There are several hints obtained from the results presented in this work that point to a role of proteins in the pPC platform formation. The exact partner within the huge number of proteinshas not been established. One can only speculate about this missing link.

The results obtained from intracellular calcium increase suggest a possible electrostatic influence. This influence was already observed on protein cluster formations (Zilly et al., 2011). The distortion of the protein cluster formation by calcium ions seems to have an effect on the number of labeled pPC spots.

Experiments with StarD2 treatment of plasma membranes might be useful to clarify if the protein/lipid complex can be destabilized by depletion of pPC from the PM pool. The decrease in concentration of pPC on the PM should have a direct effect on the formation of pPC platforms.Even though half of the pPC was depleted from the membrane (100 nM StarD2 treatment) platforms were still present. This points to a strong recruiting role of proteins, but it is unclear if the enrichment factor is the same. It is necessary to continue exploiting the possibilities that lipid transfer proteins offer.

Furthermore, the trypsin experiment directly demonstrates that the pPC spots formed within the PM of cells must be connected to a protein (or a protein complex). The liberation of the platforms as floating entities on the PM is a remarkable observation. The enzyme cuts in unspecific manner many proteins removing a possible provided anchorage system. Even a connection to cytoskeletal proteins might be possible. PC spots could represent the basement of the pillars that connect and support cytoskeleton localized in intimate contact with the inner leaflet of the PM.

The exact mechanism of PC platform formation can only be understood after clarifying and detecting the exact protein partners and the information so far is not sufficient for clarifying the yet unknown local function and the role of PC platforms at the basic level. A biological importance of PC domains is also unknown and can only be speculated on.

4.5 Model of PC organization within the PM

For illustration of PC packing within the pPC spots, a model was composed from the data obtained so far by experimental results of this work in combination with information gained from studies that analyzed the specific composition of vesicles (Takamori et al., 2006) and the assumption that PC makes up 40 % of the lipids found in plasma membranes (van Meer et al., 2008).The characterization of the pPC platforms performed in this work and the addition of the mentioned knowledge helped to generate the model presented in figure 35.

In summary, pPC platforms have a size of 120 nm and enrichment of pPC (around 200 %) suggests that within platforms 20,000 pPC molecules cover around 50 % of the structure.

This model was calculated based on the characteristics of pPC. The total amount of molecules is probably an underestimate because of the self-quenching effect between tightly packed dyes. Nevertheless, it is concluded that in the platforms pPC molecules are packed in high densities forming a novel lipid arrangement.
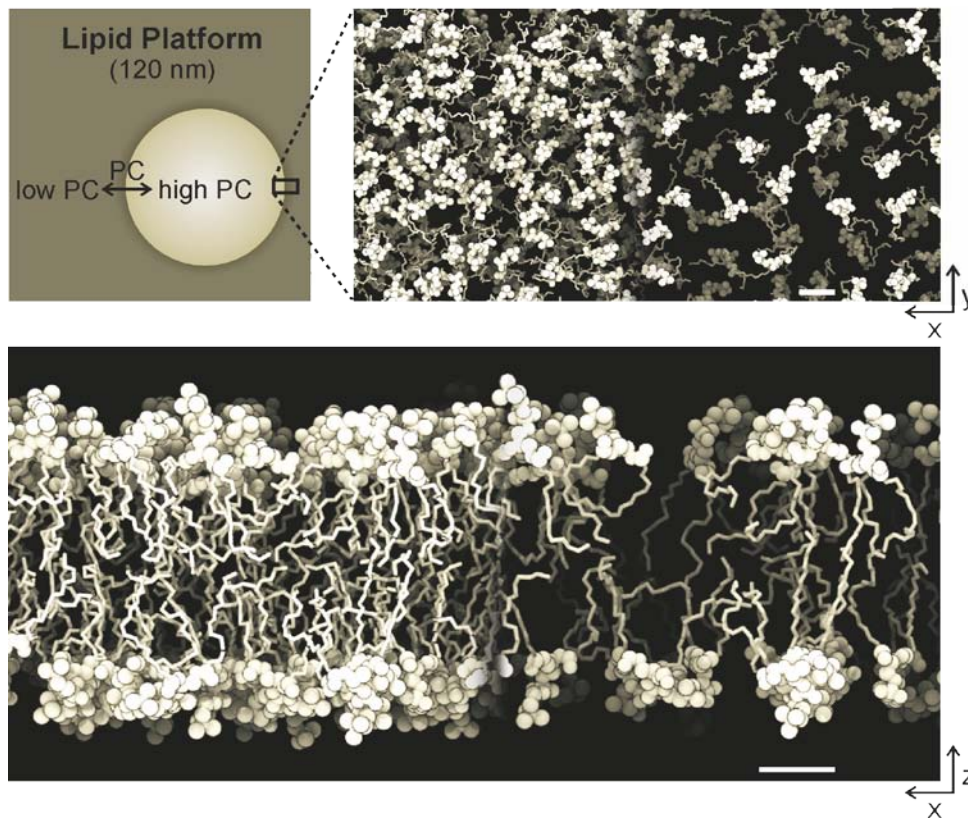
Figure 35.Model of PC platforms on the PM of cells. Scale bar represents 1 nm.Upper right panel demonstrates the region that is focused by the upper right panel. The region viewed has a total length of around 15 nm. The transition of loose packing of pPC and the initial region of the pPC platform can be visualized from top view. Lower panel demonstrates in a sectional view the order of pPC within the PM- again the transition section and the edge of a platform are shown (Figure kindly provided by T.L. and C.K. Modified from Spitta et al., 2012).

5. Outlook

The results shown in the present work demonstrate a new organization form of the lipid phosphatidylcholine. A long standing question in cell biology, namely whether lipid platforms exist in biological membranes, has been solved. As shown using PC as an example, PC platforms 120 nm large and contain about 20,000 molecules that cover 50 % of its surface.

In order to expand the knowledge of its biological relevance it is important to perform further experiments. For example, by utilizing photoactivation localization microscopy (PALM) it should be possible to quantify theexact number of lipids that are available in such a PC spot. This nanoscale analyses have been already successfully applied when describing protein clusters (Lang and Rizzoli, 2010). Second, the protein system that lies under the formation of such spots and stabilizes this spots has to be identified. Further colocalization analysis with markers of proteins that are involved with the cytoskeleton should be performed (e.g. using phalloidin staining or actin staining). Third, the lipid transfer proteins that are specific in binding will provide a toolbox that enables a manipulation in concentrations of the lipid composition of membranes and therefore analysis on membrane sheets as already shown in this work will help to understand the role of lipid proteins interactions where knowledge is still very limited. In the end, by understanding the exact mechanism of platform formation, it will be also possible to find out the biological role of such lipid platforms.

6. Literature

Akira, S., and Takeda, K. (2004).Toll-like receptor signalling. Nat. Rev. Immunol. 4, 499-511.

Alberts, B. (2008).Molecular biology of the cell. 5. Ed. New York: Garland Science. 619, 630.

Aloia, R. (1983). Membrane fluidity in biology.Vol. 2.Academic Press, 119.

Alpy, F., and Tomasetto, C. (2005). Give lipids a START: the StAR-related lipid transfer (START) domain in mammals. J. Cell. Sci. 118, 2791-2801.

Avery, J., Ellis, D.J., Lang, T., Holroyd, P., Riedel, D., Henderson, R.M., Edwardson, J.M., and Jahn, R. (2000).A cell-free system for regulated exocytosis in PC12 cells.J. Cell Biol. 148, 317-324.

Bar-On, D., Wolter, S., van de Linde, S., Heilemann, M., Nudelman, G., Nachliel, E., Gutman, M., Sauer, M., and Ashery, U. (2012). Super-resolution Imaging Reveals the Internal Architecture of Nano-sized Syntaxin Clusters. J. Biol. Chem. 287, 27158-27167.

Batista, A.P., Marreiros, B.C., and Pereira, M.M. (2012).The role of proton and sodium ions in energy transduction by respiratory complex I. IUBMB Life 64, 492-498.

Bill, A., Schmitz, A., Albertoni, B., Song, J.-N., Heukamp, L.C., Walrafen, D., Thorwirth, F., Verveer, P.J., Zimmer, S., and Meffert, L., et al. (2010). Cytohesins are cytoplasmic ErbB receptor activators. Cell 143, 201-211.

Blom, T., Somerharju, P., and Ikonen, E. (2011).Synthesis and biosynthetic trafficking of membrane lipids.Cold Spring Harb Perspect Biol 3 (8).

Cha, B., Kenworthy, A., Murtazina, R., and Donowitz, M. (2004). The lateral mobility of NHE3 on the apical membrane of renal epithelial OK cells is limited by the PDZ domain proteins NHERF1/2, but is dependent on an intact actin cytoskeleton as determined by FRAP. J. Cell. Sci. 117, 3353-3365.

Chamber, B.E., Knowles, B.R. (1976).A solvent system for delipidation of plasma or serum without protein precipitation. J. Lipid Res. 2, 176-181.

Chamberlain, L.H., and Gould, G.W. (2002). The vesicle- and target-SNARE proteins that mediate Glut4 vesicle fusion are localized in detergent-insoluble lipid rafts present on distinct intracellular membranes. J. Biol. Chem. 277, 49750-49754.

Danielli, J.F., Davson, H. (1935).A contribution to the theory of permeability of thin films.J. Cell. Comp. Physiol 5 (4), 495–508.

Denker, A., Bethani, I., Kröhnert, K., Körber, C., Horstmann, H., Wilhelm, B.G., Barysch, S.V., Kuner, T., Neher, E., and Rizzoli, S.O. (2011). A small pool of vesicles maintains synaptic activity in vivo. Proc. Natl. Acad. Sci. U.S.A. 108, 17177-17182.

Edidin, M. (2001). Membrane cholesterol, protein phosphorylation, and lipid rafts. Sci. STKE 2001, pe1.

Eggeling, C., Ringemann, C., Medda, R., Schwarzmann, G., Sandhoff, K., Polyakova, S., Belov, V.N., Hein, B., Middendorff, C. von, and Schönle, A.(2009). Direct observation of the nanoscale dynamics of membrane lipids in a living cell. Nature 457, 1159-1162.

Engelman, D.M. (2005). Membranes are more mosaic than fluid. Nature 438, 578-580.

Faugeras, P., Boens, B., Elchinger, P., Brouillete, F., Montplaisir, D., Zerrouki, R., and Lucas, R. (2012).When Cyclodextrins Meet Click Chemistry.Eur. J. Org. Chem., 4087-4105.

Foster, L.J., Hoog, C.L. de, and Mann, M. (2003). Unbiased quantitative proteomics of lipid rafts reveals high specificity for signaling factors. Proc. Natl. Acad. Sci. U.S.A. 100, 5813-5818.

Fox, C.H., Johnson, F.B., Whiting, J., and Roller, P.P. (1985).Formaldehyde fixation. J. Histochem. Cytochem.33, 845-853.

Frye, L.D., and Edidin, M. (1970).The rapid intermixing of cell surface antigens after formation of mouse-human heterokaryons. J. Cell. Sci. 7, 319-335.

Fujimoto, T., Lee, K., Miwa, S., and Ogawa, K. (1991). Immunocytochemical localization of fodrin and ankyrin in bovine chromaffin cells in vitro. J. Histochem. Cytochem. 39, 1485-1493.

Fujiwara, T., Ritchie, K., Murakoshi, H.,Jacobson, K., Kusumi, A. (2002). Phospholipids undergo hop diffusion in compartmentalized cell membrane. J Cell Biol 157 (6), 1071–1081.

Gibellini, F., and Smith, T.K. (2010).The Kennedy pathway--De novo synthesis of phosphatidylethanolamine and phosphatidylcholine. IUBMB Life 62, 414-428.

Gorter, E., and Grendel, F. (1925).Onbiomolecularlayersoflipoidsonthechromocytesof theblood.J. Exp. Med 41, 439-443.

Guhr, E. (2005). Die StarD-Proteinfamilie: Lokalisierung und Interaktion mit Lipiden. BSc. thesis (Zittau).

Gupta, N., and DeFranco, A.L. (2007). Lipid rafts and B cell signaling. Semin. Cell Dev. Biol. 18, 616-626.

Hancock, J.F. (2006). Lipid rafts: contentious only from simplistic standpoints. Nat. Rev. Mol. Cell Biol. 7, 456-462.

He, H.-T., and Marguet, D. (2011).Detecting nanodomains in living cell membrane by fluorescence correlation spectroscopy. Annu Rev Phys Chem 62, 417-436.

Heerklotz, H. (2002). Triton promotes domain formation in lipid raft mixtures. Biophys J 83 (5), 2693–2701.

Hell, S.W., and Wichmann, J. (1994). Breaking the diffraction resolution limit by stimulated emission: stimulated-emission-depletion fluorescence microscopy.Opt Lett 19, 780-782.

Holzer, R.G., Park, E.-J., Li, N., Tran, H., Chen, M., Choi, C., Solinas, G., and Karin, M. (2011). Saturated fatty acids induce c-Src clustering within membrane subdomains, leading to JNK activation. Cell 147, 173-184.

Hooke, R. (1664).Micrographia.Some physiological descriptions of minute bodies made by magnifying glasses with observations and inquiries thereupon.London: Royal Society.

Hub, J.S., Winkler, F.K., Merrick, M., and Groot, B.L. de (2010). Potentials of mean force and permeabilities for carbon dioxide, ammonia, and water flux across a Rhesus protein channel and lipid membranes. J. Am. Chem. Soc. 132, 13251-13263.

Jacobson, K., Mouritsen, O.G., and Anderson, R.G.W. (2007). Lipid rafts: at a crossroad between cell biology and physics. Nat. Cell Biol. 9, 7-14.

Jao, C.Y. Roth, M., Welti, R., and Salic, A. (2009).Metabolic labeling and direct imaging of choline phospholipids in vivo. Proc. Natl. Acad. Sci. U.S.A. 106, 15332-15337.

Jesorka, A., Orwar, O. (2008). Liposomes: technologies and analytical applications. Annu Rev Anal Chem (Palo Alto Calif) 1, 801–832.

Kanno, K., Wu, M.K., Scapa, E.F., Roderick, S.L., and Cohen, D.E. (2007).Structure and function of phosphatidylcholine transfer protein (PC-TP)/StarD2.Biochim.Biophys. Acta 1771, 654-662.

Knowles, M.K., Barg, S., Wan, L., Midorikawa, M., Chen, X., and Almers, W. (2010). Single secretory granules of live cells recruit syntaxin-1 and synaptosomal associated protein 25 (SNAP-25) in large copy numbers. Proc. Natl. Acad. Sci. U.S.A. 107, 20810-20815.

Kolb, H.C., Finn, M.G., and Sharpless, K.B. (2001). Click Chemistry: Diverse Chemical Function from a Few Good Reactions. Angew. Chem. Int. Ed. Engl. 40, 2004-2021.

Kusumi, A., Sako, Y., Yamamoto, M. (1993).Confined lateral diffusion of membrane receptors as studied by single particle tracking (nanovid microscopy). Effects of calcium-induced differentiation in cultured epithelial cells. Biophys J 65 (5), 2021–2040.

Kusumi, A., and Suzuki, K. (2005).Toward understanding the dynamics of membrane-raft-based molecular interactions.Biochim.Biophys. Acta 1746, 234-251.

Kusumi, A., Nakada, C., Ritchie, K., Murase, K., Suzuki, K., Murakoshi, H., Kasai, R.S., Kondo, J., and Fujiwara, T. (2005). Paradigm shift of the plasma membrane concept from the two-dimensional continuum fluid to the partitioned fluid: high-speed single-molecule tracking of membrane molecules. Annu Rev Biophys Biomol Struct 34, 351-378.

Kyhse-Andersen, J. (1984). Electroblotting of multiple gels: a simple apparatus without buffer tank for rapid transfer of proteins from polyacrylamide to nitrocellulose. J. Biochem. Biophys. Methods 10, 203-209.

Lang, T., Bruns, D., Wenzel, D., Riedel, D., Holroyd, P., Thiele, C., and Jahn, R. (2001). SNAREs are concentrated in cholesterol-dependent clusters that define docking and fusion sites for exocytosis. EMBO J. 20, 2202-2213.

Lang, T. (2003).Imaging SNAREs at work in 'unroofed' cells-approaches that may be of general interest for functional studies on membrane proteins.Biochem. Soc. Trans 31 (Pt 4), 861–864.

Lang, T. (2007).SNARE proteins and 'membrane rafts'. J. Physiol. (Lond.) 585, 693-698.

Lang, T., and Rizzoli, S.O. (2010). Membrane protein clusters at nanoscale resolution: more than pretty pictures. Physiology (Bethesda) 25, 116-124.

Li, Z., and Vance, D.E. (2008).Phosphatidylcholine and choline homeostasis. J. Lipid Res. 49, 1187-1194.

Lingwood, D., and Simons, K. (2010). Lipid rafts as a membrane-organizing principle. Science 327, 46-50.

Manders, E.M., Stap, J., Brakenhoff, G.J., van Driel, R., and Aten, J.A. (1992). Dynamics of three-dimensional replication patterns during the S-phase, analysed by double labelling of DNA and confocal microscopy. J. Cell. Sci. 103 (Pt 3), 857-862.

Mattheyses, A.L., Simon, S.M., and Rappoport, J.Z. (2010).Imaging with total internal reflection fluorescence microscopy for the cell biologist. J. Cell. Sci. 123, 3621-3628.

McIntosh, A.L., Storey, S.M., and Atshaves, B.P. (2010). Intracellular lipid droplets contain dynamic pools of sphingomyelin: ADRP binds phospholipids with high affinity. Lipids 45, 465-477.

McNeil, P.L., and Steinhardt, R.A. (2003). Plasma membrane disruption: repair, prevention, adaptation. Annu. Rev. Cell Dev. Biol. 19, 697-731.

Meijering, E., Dzyubachyk, O., and Smal, I. (2012).Methods for cell and particle tracking.Meth.Enzymol. 504, 183-200.

Mishra, S., and Joshi, P.G. (2007). Lipid raft heterogeneity: an enigma. J. Neurochem. 103 Suppl 1, 135-142.

Morandat, S., Azouzi, S., Beauvais, E., Mastouri, A., and El Kirat, K. (2012).Atomic force microscopy of model lipid membranes.Anal Bioanal Chem.

Morone, N., Fujiwara, T., Murase, K., Kasai, R.S., Ike, H., Yuasa, S., Usukura, J., and Kusumi, A. (2006). Three-dimensional reconstruction of the membrane skeleton at the plasma membrane interface by electron tomography. J. Cell Biol. 174, 851-862.

Morone, N., Nakada, C., Umemura, Y., Usukura, J., and Kusumi, A. (2008). Three-dimensional molecular architecture of the plasma-membrane-associated cytoskeleton as reconstructed by freeze-etch electron tomography. Methods Cell Biol. 88, 207-236.

Mueller V, Ringemann C, Honigmann A, Schwarzmann G, Medda R, Leutenegger M, Polyakova S, Belov VN, Hell SW, Eggeling C. (2011) STED nanoscopy reveals molecular details of cholesterol- and cytoskeleton-modulated lipid interactions in living cells. Biophys. J. 101:1651–1660.

Murray, D.H., and Tamm, L.K. (2011).Molecular mechanism of cholesterol- and polyphosphoinositide-mediated syntaxin clustering.Biochemistry 50, 9014-9022.

Nakamura, K., Watakabe, A., Hioki, H., Fujiyama, F., Tanaka, Y., Yamamori, T., and Kaneko, T. (2007).Transiently increased colocalization of vesicular glutamate transporters 1 and 2 at single axon terminals during postnatal development of mouse neocortex: a quantitative analysis with correlation coefficient.Eur. J. Neurosci. 26, 3054-3067.

Nelson, D.L., Cox, M.M., Lehninger, A.L. (2001).Principles of biochemistry. 3. Ed. Berlin: Springer.

Ohtsubo, K., and Marth, J.D. (2006).Glycosylation in cellular mechanisms of health and disease.Cell 126, 855-867.

Overton, C. (1895). Über die osmotischen Eigenschaften der lebenden Pflanzen- und Tierzelle. Fäsi & Beer.

Owen, D.M., Williamson, D., Magenau, A., and Gaus, K. (2012). Optical techniques for imaging membrane domains in live cells (live-cell palm of protein clustering).Meth.Enzymol. 504, 221-235.

Pearse, B.M. (1976). Clathrin: a unique protein associated with intracellular transfer of membrane by coated vesicles. Proc. Natl. Acad. Sci. U.S.A. 73, 1255-1259.

Phillips, R., Ursell, T., Wiggins, P., and Sens, P. (2009). Emerging roles for lipids in shaping membrane-protein function. Nature 459, 379-385.

Pike, L.J. (2006). Rafts defined: a report on the Keystone Symposium on Lipid Rafts and Cell Function. J. Lipid Res. 47, 1597-1598.

Pörn, M.I., Ares, M.P., and Slotte, J.P. (1993). Degradation of plasma membrane phosphatidylcholine appears not to affect the cellular cholesterol distribution. J. Lipid Res. 34, 1385-1392.

Qian, H., Sheetz, M.P., and Elson, E.L. (1991).Single particle tracking.Analysis of diffusion and flow in two-dimensional systems.Biophys. J. 60, 910-921.

Quinn, P.J., Tessier, C., Rainteau, D., Koumanov, K.S., and Wolf, C. (2005). Structure and thermotropic phase behaviour of detergent-resistant membrane raft fractions isolated from human and ruminant erythrocytes. Biochim.Biophys. Acta 1713, 5-14.

Quinn, P. J. (2010). A lipid matrix model of membrane raft structure. Prog. Lipid Res 49 (4), 390–406.

Robertson, J. D. (1981).Membrane structure. J Cell Biol 91 (3 Pt 2), 189-204.

Roderick, S.L., Chan, W.W., Agate, D.S., Olsen, L.R., Vetting, M.W., Rajashankar, K.R., and Cohen, D.E. (2002).Structure of human phosphatidylcholine transfer protein in complex with its ligand. Nat. Struct. Biol. 9, 507-511.

Rosa, P., and Fratangeli, A. (2010).Cholesterol and synaptic vesicle exocytosis. Commun Integr Biol 3, 352-353.

Rostovtsev, V.V., Green, L.G., Fokin, V.V., and Sharpless, K.B. (2002). A stepwise huisgen cycloaddition process: copper(I)-catalyzed regioselective "ligation" of azides and terminal alkynes. Angew.Chem. Int. Ed. Engl. 41, 2596-2599.

Sahl, S.J., Leutenegger, M., Hilbert, M., Hell, S.W., and Eggeling, C. (2010). Fast molecular tracking maps nanoscale dynamics of plasma membrane lipids. Proc. Natl. Acad. Sci. U.S.A. 107, 6829-6834.

Saleem, Q., Lai, A., Morales, H.H., and Macdonald, P.M. (2012). Lateral diffusion of bilayer lipids measured via ^{31}P CODEX NMR. Chem. Phys. Lipids 165, 721-730.

Sambrook, J., Rusell, D. (2006). The condensed protocols from molecular cloning. A laboratory manual (Cold Spring Harbor Laboratory Press).

Schleiden, M. J. (1838).Beiträge zur Phytogenesis. Berlin: Archiv für Anatomie, Physiologie und wissenschaftliche Medicin.

Schneider, C.A., Rasband, W.S., Eliceiri, K.W. (2012).NIH Image to ImageJ: 25 years of image analysis. Nat Meth 9 (7), 671–675.

Schreiber, A., Fischer, S., and Lang, T. (2012). The amyloid precursor protein forms plasmalemmal clusters via its pathogenic amyloid-β domain. Biophys. J. 102, 1411-1417.

Schwann, T., Smith, H., Schleiden, M.J. (1847).Microscopical researches into the accordance in the structure and growth of animals and plants: The Sydenham Society.

Sheetz, M.P., Schindler, M., and Koppel, D.E. (1980). Lateral mobility of integral membrane proteins is increased in spherocytic erythrocytes. Nature 285, 510-511.

Shogomori, H.; Brown, D.A. (2003). Use of detergents to study membrane rafts: the good, the bad, and the ugly. Biol Chem 384 (9), 1259–1263.

Sieber, J.J., Willig, K.I., Heintzmann, R., Hell, S.W., and Lang, T. (2006). The SNARE motif is essential for the formation of syntaxin clusters in the plasma membrane. Biophys. J. 90, 2843-2851.

Sieber, J.J., Willig, K.I., Kutzner, C., Gerding-Reimers, C., Harke, B., Donnert, G., Rammner, B., Eggeling, C., Hell, S.W., and Grubmüller, H., et al. (2007). Anatomy and dynamics of a supramolecular membrane protein cluster. Science 317, 1072-1076.

Sieber, J.J., Willig, K.I., Kutzner, C., Gerding-Reimers, C., Harke, B., Donnert, G. et al. (2007). Anatomy and dynamics of a supramolecular membrane protein cluster. Science 317 (5841), 1072–1076.

Simons, K., Ikonen, E. (1997). Functional rafts in cell membranes. Nature 387 (6633), 569–572.

Simons, K., Gerl, M.J. (2010). Revitalizing membrane rafts: new tools and insights. Nat Rev Mol Cell Biol 11 (10), 688–699.

Simons, K., and Sampaio, J.L. (2011).Membrane Organization and Lipid Rafts.Cold Spring Harbor Perspectives in Biology 3.

Singer, S.J., and Nicolson, G.L. (1972).The fluid mosaic model of the structure of cell membranes. Science 175, 720-731.

Sowa, G. (2012). Caveolae, caveolins, cavins, and endothelial cell function: new insights. Front Physiol 2, 120.

Spitta, L., Merklinger, E., Saka-Kirli, S., Schloetel, J.-G., Lauria, I., Schmidt, T., Kandt, C., Rizzoli, S.T.C., and Lang, T. (2012). Long-lived lipid platforms in native membranes.(submitted)

Steyer, J.A., Almers, W. (2001).A real-time view of life within 100 nm of the plasma membrane. Nat. Rev. Mol. Cell Biol 2 (4), 268–275.

Stocco, D.M. (2001). StAR protein and the regulation of steroid hormone biosynthesis. Annu. Rev. Physiol. 63, 193-213.

Takamori, S., Holt, M., Stenius, K., Lemke, K.A., Grønborg, M., Riedel, D., Urlaub, H., Schenck, S., Brügger, B., and Ringler, P. (2006). Molecular anatomy of a trafficking organelle. Cell 127, 831-846.

Thiele.C., Papan, C., Hoelper D., Kusserow, K., Gaebler, A., Schoene, M., Piotrowitz, K., Lohmann, D., Spandl J., and Stevanovic, A., et al. (2012).Tracing fatty acid metabolism by click-chemistry. ACS Chem. Biol.

Thompson, N.L., Lieto, A.M., and Allen, N.W. (2002). Recent advances in fluorescence correlation spectroscopy. Curr.Opin.Struct. Biol. 12, 634-641.

Tian, X., Pai, J., and Shin, I. (2012).Analysis of density-dependent binding of glycans by lectins using carbohydrate microarrays. Chem Asian J 7, 2052-2060.

Tsuji, A., and Ohnishi, S. (1986). Restriction of the lateral motion of band 3 in the erythrocyte membrane by the cytoskeletal network: dependence on spectrin association state. Biochemistry 25, 6133-6139.

Uhles, S., Moede, T., Leibiger, B., Berggren, P.-O., and Leibiger, I.B. (2003). Isoform-specific insulin receptor signaling involves different plasma membrane domains. J. Cell Biol. 163, 1327-1337.

van Meer, G., Voelker, D.R., and Feigenson, G.W. (2008). Membrane lipids: where they are and how they behave. Nat. Rev. Mol. Cell Biol. 9, 112-124.

van Meer, G., and Kroon, A.I.P.M. de (2011). Lipid map of the mammalian cell.J. Cell. Sci. 124, 5-8.

Virchow, R.L.K. (1871). Die Cellularpathologiein in ihrer Begründung auf physiologische und pathologische Gewebelehre.2. Ed. Berlin: published by A. Hirschwald.

Wawrezinieck, L., Rigneault, H., Marguet, D., and Lenne, P.-F.(2005). Fluorescence correlation spectroscopy diffusion laws to probe the submicron cell membrane organization.Biophys. J. 89, 4029-4042.

Wenger, J., Conchonaud, F., Dintinger, J., Wawrezinieck, L., Ebbesen, T.W., Rigneault, H., Marguet, D., and Lenne, P.-F. (2007). Diffusion analysis within single nanometric apertures reveals the ultrafine cell membrane organization. Biophys. J. 92, 913-919.

Williams, T.M., and Lisanti, M.P. (2004).The caveolin proteins.Genome Biol. 5, 214.

Xu, X., and London, E. (2000). The effect of sterol structure on membrane lipid domains reveals how cholesterol can induce lipid domain formation. Biochemistry 39, 5351-5361.

Yang, M., Song, Y., Zhang, M., Lin, S., Hao, Z., Liang, Y., Zhang, D., and Chen, P.R. (2012).Converting a solvatochromic fluorophore into a protein-based pH indicator for extreme acidity.Angew.Chem. Int. Ed. Engl. 51, 7674-7679.

Zacharias, D.A., Violin, J.D., Newton, A.C., and Tsien, R.Y. (2002).Partitioning of lipid-modified monomeric GFPs into membrane microdomains of live cells.Science 296, 913-916.

Zilly, F.E., Halemani, N.D., Walrafen, D., Spitta, L., Schreiber, A., Jahn, R., Lang, T. (2011).Ca2+ induces clustering of membrane proteins in the plasma membrane via electrostatic interactions. EMBO J 30 (7), 1209–1220.

Zurzolo, C., van Meer, G., and Mayor, S. (2003). The order of rafts.Conference on microdomains, lipid rafts and caveolae. EMBO Rep. 4, 1117-1121.